Toxicon xxx (xxxx) xxx

Contents lists available at ScienceDirect

Toxicon

journal homepage: www.elsevier.com/locate/toxicon

Functional venom activity and antivenom neutralization in rattlesnakes across Baja California and Gulf of California islands

Samuel R. Hirst [a,*,1], Edgar Neri-Castro [b,**,1], Emiliano Vázquez-García [b], Vanessa Zarzosa [b], Felipe Olvera [b], Cameron M. VanHorn [a], Alejandro Alagón [b], Hector Franz-Chávez [c], Gamaliel Castañeda-Gaytán [d], Christopher L. Parkinson [e], Jason L. Strickland [f], Miguel Borja [d], Mark J. Margres [a]

[a] University of South Florida, Department of Integrative Biology, 12037 USF Beard Drive, Tampa, 33620, FL, USA
[b] Universidad Nacional Autónoma de México, Departamento de Medicina Molecular y Bioprocesos, Av. Universidad 2001, Cuernavaca, 62210, Mor., Mexico
[c] Herp.MX©, Colima, Colima, Mexico
[d] Universidad Juárez del Estado de Durango, Facultad de Ciencias Biológicas, Av. Universidad s/n., Gómez Palacio, 35010, Dgo., Mexico
[e] Clemson University, Department of Biological Sciences, 132 Long Hall, Clemson, 29631, SC, USA
[f] University of South Alabama, Department of Biology, 5871 USA Dr., Mobile, 36688, AL, USA

ARTICLE INFO

Handling Editor: Bruno Lomonte

Keywords:
Fibrinogenolytic activity
PLA_2
Venom neutralization
Proteolysis
Lethality

ABSTRACT

Snake venoms are complex biochemical phenotypes whose composition can diverge dramatically among taxa, yet the functional and biomedical consequences of such variation remain understudied for many lineages. Here, we characterized the functional activities of venom from multiple rattlesnake species distributed across insular and mainland localities in the Baja California Peninsula and Gulf of California. We quantified phospholipase A_2 (PLA_2), proteolytic, and fibrinogenolytic activities as well as median lethal doses (LD_{50}) for 55 individuals across *Crotalus enyo*, *C. mitchellii*, *C. pyrrhus sensu lato*, and *C. ruber*. We also evaluated the neutralization efficacy of the commercial polyvalent antivenom Antivipmyn®. Venom functional activities differed significantly among species. *Crotalus mitchellii* expressed a neurotoxic phenotype characterized by the highest PLA_2 activity, the lowest LD_{50} values, and minimal proteolysis. *Crotalus pyrrhus* and *C. ruber* expressed proteolytic phenotypes with high enzymatic activity and ubiquitous dual-chain fibrinogenolysis. *Crotalus enyo* exhibited intermediate functional activities with moderate enzymatic output and the most efficient antivenom neutralization among species. Although Antivipmyn® neutralized the lethal activity of all venoms, efficacy differed significantly among species in both mass-normalized (mgAV/mgV) and potency-scaled (LD_{50}-equivalents per vial) metrics. Notably, insular and mainland populations within species showed qualitative variation in both functional activities and antivenom responses. These results establish that the focal species possess functionally distinct venom phenotypes with species-specific consequences for antivenom neutralization, underscoring the relevance of venom functional characterization for clinical management of envenomation across the Baja California region.

1. Introduction

Snake venoms are complex biochemical phenotypes composed of 40–100 proteins and peptides that collectively mediate prey immobilization, digestion, and defense (Daltry et al., 1996; Barlow et al., 2009; Casewell et al., 2011; Munawar et al., 2018; Mackessy, 2021). Venom composition often varies extensively among species (Glenn and Straight, 1985; Casewell et al., 2014; Margres et al., 2015b; Jackson and Fry, 2016; Jackson et al., 2016; Durban et al., 2017; Pla et al., 2019; Senji Laxme et al., 2019; Holding et al., 2021; Borja et al., 2025; Hirst et al., 2025), populations (Massey et al., 2012; Margres et al., 2015b; Holding et al., 2018; Margres et al., 2019; Smith et al., 2023; Hirst et al., 2024, 2025), and individuals across ontogeny (Andrade and Abe, 1999; Alape-Girón et al., 2008; Barlow et al., 2009; Margres

* Correspondence to: Columbia University, Department of Ecology, Evolution, and Environmental Biology, 51200 Amsterdam Avenue, New York, 10027, NY, USA.
** Corresponding author.
E-mail addresses: hirsts@usf.edu (S.R. Hirst), edgar.neri@ibt.unam.mx (E. Neri-Castro).
[1] These authors contributed equally to this work and share first authorship.

https://doi.org/10.1016/j.toxicon.2026.109266
Received 18 June 2026; Received in revised form 11 August 2026; Accepted 11 August 2026
Available online 31 August 2026

et al., 2015b,a; Wray et al., 2015; Modahl et al., 2016; Durban et al., 2017; Rokyta et al., 2017; Cipriani et al., 2017; Borja et al., 2018; Schonour et al., 2020; Hirst et al., 2024; Borja et al., 2025). Despite this well-documented compositional diversity, the functional consequences of venom variation often remain less explored. Because snake venom is predominantly a trophic adaptation, its functional properties are shaped by the physiological characteristics of prey species (Daltry et al., 1996; Barlow et al., 2009; Holding et al., 2016; Smiley-Walters et al., 2017; Holding et al., 2021). Selection favors venom phenotypes that efficiently incapacitate prey with particular biochemical and physiological defenses; therefore dietary shifts can drive divergence in venom composition and function (Barlow et al., 2009; Holding et al., 2016; Margres et al., 2017b; Smiley-Walters et al., 2017; Casewell et al., 2020; Mackessy, 2021; Holding et al., 2026). Historically in rattlesnakes, the most divergent venom phenotypes have been categorized using the Type A and Type B dichotomy, which distinguishes between highly lethal, neurotoxic A venoms and B venoms characterized by low lethality and high proteolytic activity (Glenn and Straight, 1978; Glenn et al., 1983). This framework was further refined into the Type I and Type II classification system to describe the fundamental inverse relationship between metalloproteinase activity and systemic lethality (Mackessy, 2010). Under this model, Type I (roughly corresponding to Type B) venoms emphasize tissue-destructive proteolysis, whereas Type II (Type A) venoms prioritize systemic toxicity. However, these categories represent ends of a functional continuum rather than discrete states; intermediate phenotypes (Type I+II) exist (Mackessy, 2010; Strickland et al., 2018; Colis-Torres et al., 2022), utilizing both neurotoxic and proteolytic strategies. This biochemical gradient directly impacts the clinical manifestations of envenomation, as shifts in the balance of these toxin families can influence both the pathophysiology of the bite and the efficacy of antivenom neutralization (Calvete, 2010; Casewell et al., 2014).

Recent work has demonstrated that venom protein expression across populations of four rattlesnake species, the Baja California Rattlesnake (*Crotalus enyo*), Red Diamond Rattlesnake (*C. ruber*), Speckled Rattlesnake (*C. mitchellii*), and Southwestern Speckled Rattlesnake (*C. pyrrhus sensu lato*), from the Baja California Peninsula and adjacent Gulf of California islands was significantly variable (Hirst et al., 2024, 2025, 2026). We previously found that venom expression differed significantly across islands, with venom complexity predicted by island size, isolation, and competition (Hirst et al., 2025). Similarly, we documented geographic venom variation across the mainland range of *C. ruber* (Hirst et al., 2024) and between an island and mainland population of *C. enyo* (Hirst et al., 2026). These findings align with broader toxicological and epidemiological surveys in Baja California (Glenn and Straight, 1985; Rodríguez-Canseco et al., 2021) that have identified significant biochemical divergence among many of these same co-occurring taxa across Baja California Sur (Arnaud-Franco et al., 2018) and within specific clades, such as the speckled rattlesnake complex (Arnaud-Franco et al., 2023) and *C. ruber* (Pozas-Ocampo et al., 2020). However, we have not determined whether broad-scale variation in venom expression across the peninsula and islands translates into functional differences in venom activity and/or differences in antivenom efficacy.

Venom proteins can vary substantially in relative abundance without altering overall enzymatic activity, toxicity, or biological effects (Casewell et al., 2013; Margres et al., 2016; Gutiérrez et al., 2017; Xiong and Huang, 2018; Pucca et al., 2020; Mackessy, 2021; Rudresha et al., 2025). Consequently, differences in expression profiles alone cannot be assumed to reflect functional divergence or predict antivenom performance. Determining whether geographically variable venoms differ in their functional properties, such as phospholipase A_2 activity, proteolytic capacity, fibrinogen degradation, and lethality, is therefore essential not only for understanding the biological consequences of venom evolution, but also for evaluating the biomedical implications of venom variation for antivenom efficacy.

In Mexico, viper envenomation is treated frequently using Antivipmyn®, a commercially produced polyvalent antivenom generated against a mixture of venoms from medically important viperids, primarily *Bothrops asper* and *Crotalus durissus* (Sánchez et al., 2003; Ponce-López et al., 2020; Guadarrama-Martínez et al., 2024). Polyvalent antivenoms are designed to provide broad protection across taxa and regions, yet their efficacy can vary depending on the biochemical composition and functional properties of target venoms relative to the venoms used in production (Ratanabanangkoon, 2003; Mukherjee et al., 2016; Ratanabanangkoon, 2023). If venom function differs substantially across island and mainland populations, particularly in enzymatic activities that drive local tissue damage or systemic toxicity, this variation could influence antivenom neutralization performance (Vohra et al., 2008; Massey et al., 2012; Musick et al., 2024; Borja et al., 2025). This question is especially relevant in Baja California, a region with high levels of tourism and frequent human visitation to both mainland sites and offshore islands where the focal rattlesnake species occur (Grismer, 2002; Schmitz and Diaz, 2013; Olmos-Martínez et al., 2018).

In this study, we built directly on prior work documenting geographic variation (Glenn and Straight, 1985; Arnaud-Franco et al., 2018; Pozas-Ocampo et al., 2020; Arnaud-Franco et al., 2023; Hirst et al., 2024, 2025, 2026) in venom composition to evaluate whether that variation translates into differences in venom function and antivenom efficacy. We characterized the functional properties of venoms from four rattlesnake species sampled across insular and mainland localities, focusing on phospholipase A_2 activity, proteolytic activity, EDTA-insensitive proteolysis (i.e., the fraction of proteolytic activity resistant to metalloprotease inhibition), lethality (LD_{50}), and fibrinogenolytic activity (assessed with and without protease inhibitors). We then assessed the neutralizing performance of the commercial polyvalent antivenom Antivipmyn® using complementary mass-based and potency-scaled metrics. By linking venom functional diversity to antivenom neutralization capacity, this study provides a bridge between patterns of venom variation and their biological and clinical consequences.

2. Materials and methods

2.1. Sampling

Venom samples were collected from 55 individuals across four rattlesnake species including *Crotalus mitchellii* (n = 10), *C. ruber* (n = 14), *C. enyo* (n = 17), and *C. pyrrhus sensu lato* (n = 14). Snakes were sampled across 11 islands and six mainland regions distributed along the length of the Baja California Peninsula (Fig. 1). To maximize sample sizes for species comparisons, three insular populations of *C. pyrrhus sensu lato* that were previously described as distinct species (*C. angelensis* from Isla Ángel de la Guarda, *C. thalassoporus* from Isla Piojo, and *C. polisi* from Isla Cabeza de Caballo; Meik et al., 2018, 2015) were considered *C. pyrrhus* for this study. Snakes were located through visual encounter surveys and captured for data collection. For each individual, we recorded sampling locality, snout-vent length (SVL), and sex. Venom was extracted by allowing the snake to bite into a parafilm-covered collection cup and dried at ambient temperature under field conditions immediately upon collection. Island snakes were released at the site of capture following data collection. Mainland snakes were euthanized, dissected, vouchered, and deposited at La Colección Herpetologica de la Facultad de Ciencias Biologicas de la Universidad Juárez del Estado de Durango in Gómez Palacio, Durango, MX.

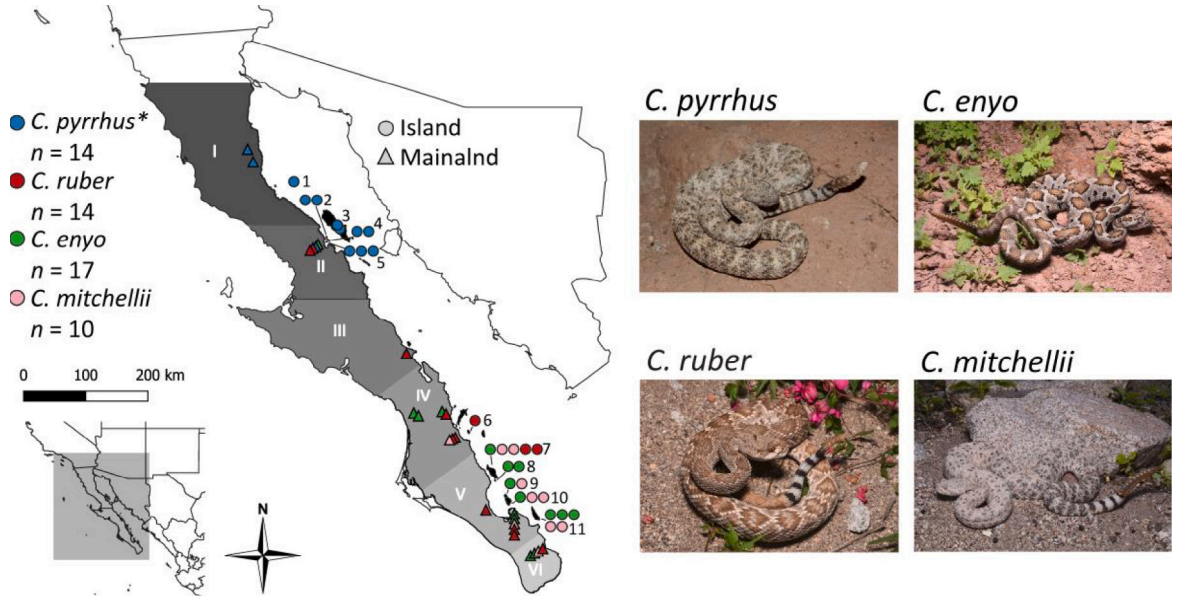

Fig. 1. Sampling of 55 rattlesnakes collected across 11 islands and six mainland regions along the Baja California Peninsula. Rattlesnakes were sampled on Isla El Muerto (1 on map; inhabited by Cp), Isla Smiths (2; Cp), Isla Angel de la Guarda (3; *Ca), Isla El Piojo (4; *Ct), Isla Cabeza de Caballo (5; *Cpo), Isla Danzante (6; Cr), Isla San Jose (7; Cm, Ce, Cr), Isla San Francisco (8; Ce), Isla Partida Sur (9; Cm, Ce), Isla Espiritu Santo (10; Cm, Ce), and Isla Cerralvo (11; Cm, Ce). Roman numerals I – VI indicate six mainland localities. Species abbreviations: Cp: *Crotalus pyrrhus*, Ce: *C. enyo*, Cm: *C. mitchellii*, Cr: *C. ruber*. Asterisks indicate insular endemics of the C. *pyrrhus* (*sensu lato*) complex: Ca: *C. angelensis*, Ct: *C. thalassoporus*, Cpo: *C. polisi*. Point color indicates species: *C. pyrrhus* (blue), *C. ruber* (red), *Crotalus enyo* (green), and *C. mitchellii* (pink); point shape indicates insular versus mainland origin. Rattlesnake image credits: Ricardo Ramírez Chaparro and Jacob Loyacano. (For interpretation of the references to color in this figure legend, the reader is referred to the web version of this article.)

2.2. Venom RP-HPLC

Venom samples were analyzed using reversed-phase high-performance liquid chromatography (RP-HPLC) as previously described (Hirst et al., 2025). Before analysis, lyophilized venom samples were resuspended in HPLC-grade water. Then, 50 μg of venom protein were injected onto a Jupiter® 5 μm C_{18} 300 Å LC column (250 × 2 mm) using a Dionex Ultimate 3000 UHPLC DAD system (Thermo Fisher Scientific). Separation was carried out with a mobile phase consisting of solvent A (0.1% trifluoroacetic acid [TFA] in water) and solvent B (0.075% TFA in acetonitrile). The chromatographic run began with 5% B for five minutes, followed by a linear gradient increasing at 1% per minute up to 25% B, then a slower increase of 0.25% per minute until reaching 65% B. The flow rate was set at 0.6 mL/min, and elution profiles were monitored at 220 nm. Chromatographic peaks were quantified using Chromeleon™ software (Thermo Fisher Scientific), with the relative abundance of each protein fraction estimated as the proportion of its peak area relative to the total chromatogram area, following established protocols (Gibbs and Rossiter, 2008; Margres et al., 2014, 2017a). Individual chromatograms and peak quantification data are provided in Supplementary Figures S1–S4 and Supplementary Table S1, respectively.

2.3. Measuring venom complexity

To quantify the diversity of venom protein expression for each individual, we calculated Shannon's diversity index (H) from the proportional RP-HPLC chromatographic peak areas using the `diversity` function from the `vegan` package in R (Shannon and Weaver, 1998; Wolf et al., 2018; Oksanen et al., 2020). Shannon's H ($H = -\sum p_i \ln p_i$, where p_i is the proportional area of the ith peak) captures both the number of detectable protein fractions and the evenness of their relative abundances, providing a continuous measure of complexity (Holding et al., 2021; Hirst et al., 2025). Higher values indicate more evenly distributed venom profiles, while lower values reflect dominance by one or a few fractions. Species-level differences in venom complexity were assessed using a Kruskal–Wallis test (see Statistical Analyses).

2.4. Protein quantification

Approximately 3–5 mg of dried venom were weighed and dissolved in 1 mL of phosphate-buffered saline (PBS). Subsequently, these samples were quantified using the bicinchoninic acid (BCA) method, as instructed by the manufacturer. Bovine serum albumin (BSA) was used to generate the standard curve. The resulting stock solutions were used for all subsequent functional assays and antivenom neutralization experiments, ensuring standardized protein concentrations across analyses.

2.5. Proteolytic activity on azocasein

Proteolytic activity was evaluated using azocasein (Sigma-Aldrich, St. Louis, MO, USA) as the substrate, based on the methodology described by Colis-Torres et al. (2022). A solution of azocasein was prepared by dissolving the substrate in buffer containing 50 mM Tris(hydroxymethyl)aminomethane hydrochloride (Tris–HCl), 0.15 M sodium chloride (NaCl), and 25 mM calcium chloride ($CaCl_2$), adjusted to pH 8.0, to achieve a final concentration of 10 mg/mL. Subsequently, 20 μg of each individual venom sample were mixed with 100 μL of the azocasein solution and incubated at 37°C for 30 min. Following incubation, 200 μL of 5% trichloroacetic acid were added to terminate the reaction, and the mixture was centrifuged at 13,000 rpm (~16,000 × g) for 5 min. A total of 150 μL of the resulting supernatant was then transferred to a 96-well plate and mixed with an equal volume (150 μL) of 0.5 M NaOH. Absorbance readings were recorded at 450 nm (Wang et al., 2004; Gutiérrez et al., 2008). All samples were tested in triplicate. Proteolytic activity was quantified as the amount of enzyme required to produce a 0.2 absorbance change per minute. The same procedure was performed using Ethylenediaminetetraacetic acid (EDTA), which can chelate zinc, thereby inhibiting metalloproteases. EDTA was used at a concentration of 5 mM as previously described (Neri-Castro et al., 2019). PBS was substituted for venom as a negative control in all assays, yielding a value of 0.02.

2.6. Fibrinogenolytic activity

Ten μg of venom were incubated with 50 μg of human fibrinogen in Eppendorf tubes at 37°C for 30 min. The resulting gel was disrupted (note that the term "gel" refers to the fibrinogen matrix formed in PBS, which develops a gelatinous consistency as a result of proteolytic degradation), and 5 μL of each incubated sample was loaded onto an SDS-PAGE under reducing conditions, with a fibrinogen sample without venom serving as a control. SDS-PAGE gels were stained with Coomassie Blue. To differentiate the activities of snake venom metalloproteinases (SVMP) and snake venom serine proteases (SVSP), the fibrinogenolytic assay was performed under four experimental conditions: (1) venom and fibrinogen, (2) venom pre-incubated with EDTA, (3) venom pre-incubated with phenylmethylsulfonyl fluoride (PMSF), and (4) venom pre-incubated with a combination of both EDTA and PMSF. These inhibitors allow for the selective inactivation of specific protease families. EDTA chelates the divalent metal ions (e.g., Zn^{2+}) required for SVMP catalytic activity, whereas PMSF covalently binds to the active-site serine residue to inhibit SVSP activity (Gené et al., 1989; Estêvão-Costa et al., 2000; Swenson and Markland, 2005; Sanchez et al., 2017; Borja et al., 2018). By comparing the resulting fibrinogen cleavage patterns across these treatments, we attributed α- and β-chain degradation to either SVMPs or SVSPs based on the presence or absence of specific chain preservation following selective inhibition. In all inhibitor treatments, venoms were pre-incubated at 37°C for 30 min prior to the addition of fibrinogen, following the procedure described by Zarzosa et al. (2024). Representative SDS-PAGE gels for all individuals across the four experimental conditions are provided in Supplementary Figures S5–S34.

2.7. Determination of PLA_2 activity using 4-NOBA substrate

The synthetic substrate 4-nitro-3-(octanoyloxy)-benzoic acid (4-NOBA) was used to assess PLA_2 activity of individual venoms, following the methodology of Holzer and Mackessy (1996). Microplate wells were filled with 200 μL of reaction buffer (10 mM Tris, 10 mM CaCl2, 0.1 M NaCl, pH 8.0) and 25 μL of substrate (4-NOBA; 1 mg/mL in acetonitrile). The reaction buffer and substrate were incubated at 37°C for 10 min, after which 20 μL of venom (1 mg/mL) were added. The mixture was then incubated at 37°C for 40 min, and absorbance was measured at 450 nm . For visualization, the raw absorbance values were multiplied by 10 (arbitrary factor). PBS was substituted for venom as a negative control, yielding a value of 0.01.

2.8. Lethality

The median lethal dose (LD_{50}) was determined using Institute of Cancer Research (ICR) mice weighing ~18–20 g; mice were kept under standardized conditions with free access to food and water (*ad libitum*). Injections were administered intravenously, with three mice used per dose (Lorke, 1983). Mortality rates were recorded 24 h post-inoculation. Data analysis was performed using Prism v10 software. A non-linear regression based on a sigmoidal dose–response curve was applied to determine the LD_{50}. Results were expressed as μg of venom per gram of mouse (Casasola et al., 2009).

2.9. Neutralization of lethal activity using commercial antivenom

The commercial antivenom Antivipmyn® (batch number B-OD-32) was used for all neutralization assays. Antivenom was confirmed to be within its validity period at the time of experimentation. According to the manufacturer, each vial is capable of neutralizing approximately 780 LD_{50} of *Bothrops asper* venom (~30 mg) and 790 LD_{50} of *Crotalus durissus* venom (~5 mg). Due to limited venom yields from several individual samples, neutralization assays were performed on a subset of the total venom collection, consisting of *C. enyo* ($n = 3$), *C. mitchellii* ($n = 7$), *C. pyrrhus* ($n = 8$), and *C. ruber* ($n = 2$). Neutralization assays were performed using a pre-incubation protocol (Lorke, 1983). Briefly, a challenge dose of three median lethal doses ($3 \times LD_{50}$) was mixed with varying volumes of antivenom and incubated at 37°C for 30 min in a final volume of 200 μL. Mixtures were administered intravenously to groups of three mice, and survival was assessed after 24 h. Dose–response curves were fitted using non-linear regression in Prism v10 (Casasola et al., 2009). Antivenom efficacy was quantified both as the mass of antivenom required to neutralize 1 mg of venom (mgAV/mgV) and as the number of median lethal dose equivalents (LD_{50}-equivalents) neutralized per vial, where each LD_{50} corresponds to the species-specific median lethal dose (Guadarrama-Martínez et al., 2024; Secretaría de Salud, 2012).

2.10. Statistical analyses

All analyses were conducted in R V4.3.2 (R Core Team, 2024). Distributions for all four venom activities were strongly right-skewed, and EDTA-insensitive proteolytic activity values (Proteolytic + EDTA) were heavily zero-inflated, with many individuals exhibiting no detectable EDTA-insensitive activity (Table 1). Given these distributional properties, unequal variances across groups, and unbalanced sampling (with several island and mainland localities represented by only one or two individuals), we used nonparametric, rank-based tests that do not assume normality, homoscedasticity, or equal group sizes and are robust to outliers.

To evaluate broad functional divergence among species, we used Kruskal–Wallis tests for the following: PLA_2 activity, total proteolytic activity, Proteolytic-EDTA, LD_{50}, antivenom neutralization, and venom complexity (Shannon H). Following each Kruskal–Wallis test, pairwise post-hoc comparisons were conducted using Dunn's test with Benjamini–Hochberg (BH) correction for multiple comparisons, as implemented in the `rstatix` package (R Core Team, 2024); complete pairwise results are provided in Supplementary Table S2. This approach allows a robust test of species-level differences without violating assumptions of normality or equal variances and accommodates the unequal sample sizes among species and localities. Because sample sizes within individual localities were often very small (frequently $n = 1-2$), we did not perform formal statistical tests of geographic variation within species (e.g., among islands or between island and mainland populations), and instead interpreted geographic patterns descriptively using locality-level summaries.

To assess potential changes in venom functional activities and antivenom neutralization across life-history (ontogeny), we performed simple linear regressions of each quantitative metric (PLA_2 activity, proteolytic activity, EDTA-insensitive proteolytic activity, LD_{50}, and venom complexity) against SVL, conducted separately per species. Antivenom metrics (mgAV/mgV and LD_{50} equivalents per vial) were assessed similarly, though statistical power was limited by small per-species sample sizes.

3. Results

3.1. Venom complexity

Venom complexity differed significantly among species (Kruskal–Wallis: H = 25.17, df = 3, P < 0.0001). Pairwise Dunn tests revealed that *C. enyo* had a significantly more complex venom than both *C. mitchellii* ($p_{adj} = 0.0015$) and *C. ruber* ($p_{adj} < 0.0001$), and that *C. pyrrhus* showed significantly higher venom complexity than *C. ruber* ($p_{adj} = 0.0064$); all other pairwise comparisons were non-significant ($p_{adj} > 0.05$; Fig. 2; Supplementary Table S2). *Crotalus enyo* venom exhibited the highest and most uniform complexity (mean 2.45; range 2.31–2.56; SD = 0.07), with little variation across island and mainland localities, indicating a relatively uniform expression of venom proteins. *Crotalus pyrrhus* showed an intermediate mean but the greatest

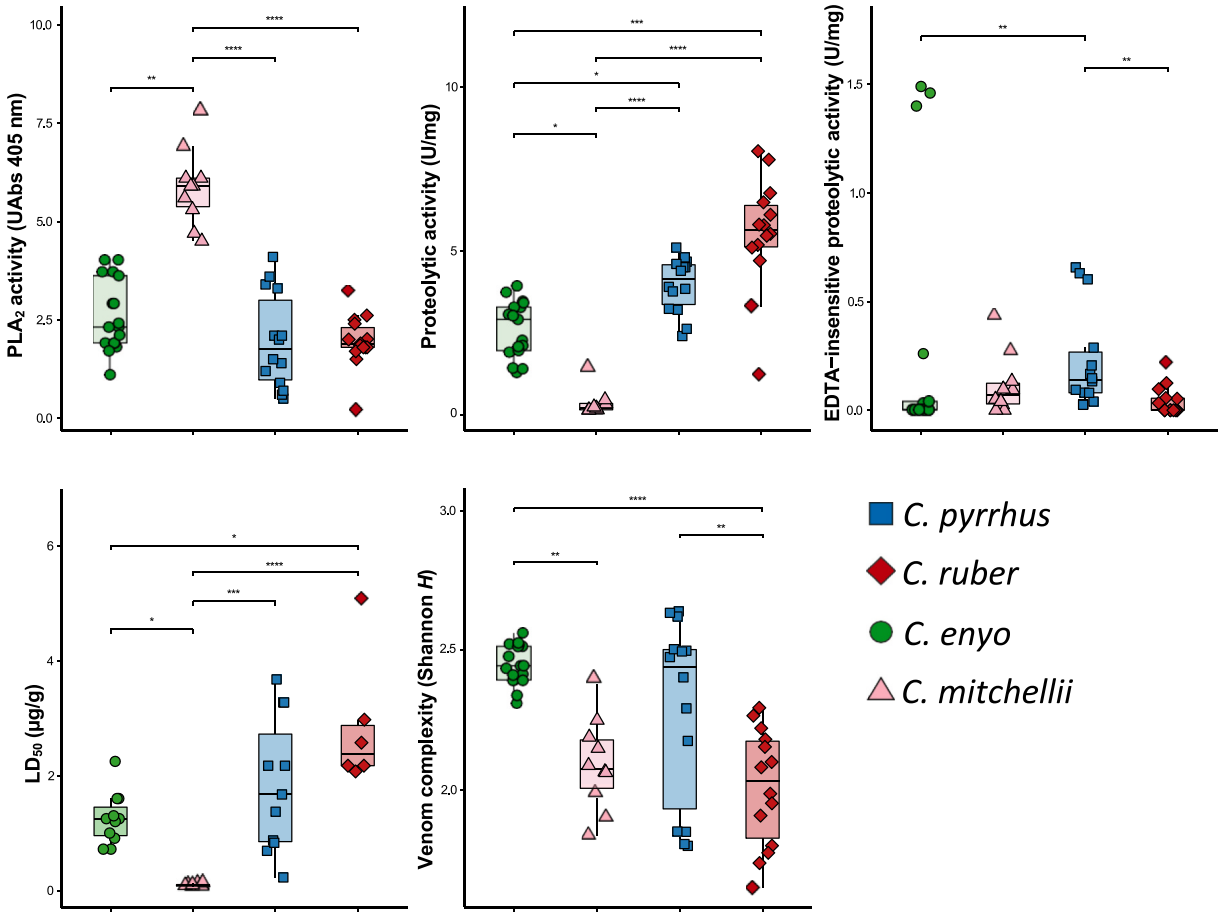

Fig. 2. Venom functional activities and complexity across four Baja California rattlesnake species. Boxplots show the median and interquartile range; individual data points are overlaid (jittered for clarity). Panels show (top row, left to right): PLA_2 activity (UAbs 405 nm), total proteolytic activity (U/mg), and EDTA-insensitive proteolytic activity (U/mg); (bottom row): median lethal dose (LD_{50}; µg venom/g mouse) and venom complexity (Shannon *H*). Species are indicated by color and shape. Significance brackets indicate pairwise Dunn test results with Benjamini–Hochberg correction: *$p < 0.05$, **$p < 0.01$, ***$p < 0.001$, ****$p < 0.0001$. Individual values and summary statistics are provided in Table 1 and Supplementary Table S2, respectively. (For interpretation of the references to color in this figure legend, the reader is referred to the web version of this article.)

among-individual variation (mean 2.29; range 1.80–2.64; SD = 0.33); complexity was notably low on Isla Ángel de la Guarda (1.81–1.86) and for one individual on Isla Cabeza de Caballo (1.80), but markedly higher on Isla Smiths (2.50–2.64) and Isla Piojo (2.18–2.51). *Crotalus mitchellii* showed lower complexity with moderate variation (mean 2.10; range 1.84–2.41; SD = 0.17), with mainland individuals from BCS IV and VI tending toward higher values than island individuals. *Crotalus ruber* venom exhibited the lowest overall complexity (mean 2.01; range 1.65–2.29; SD = 0.21), with the lowest values observed at BCS IV (San Javier; 1.65) and BCS III (San Bruno; 1.77), reflecting a venom profile dominated by a few highly abundant protein fractions (Table 1). Venom complexity was also significantly and negatively correlated with SVL in *C. ruber* ($R^2 = 0.63$, $p < 0.001$) and *C. pyrrhus* ($R^2 = 0.57$, $p = 0.002$), indicating an ontogenetic shift from more to less complex venoms over life history. No significant relationship was found in *C. enyo* or *C. mitchellii* ($p > 0.05$; Supplementary Table S4).

3.2. PLA_2 activity

PLA_2 activity varied significantly among species (Kruskal–Wallis: H = 27.23, df = 3, P < 0.001). Pairwise comparisons confirmed that *C. mitchellii* differed significantly from all other species (all $p_{adj} \leq 0.001$); all other pairwise comparisons were non-significant ($p_{adj} > 0.05$; Fig. 2; Supplementary Table S2). *Crotalus mitchellii* exhibited the highest activities, with consistently elevated values across all island and mainland localities (mean 5.88; range 4.5–7.8; SD = 1.0). In contrast, *C. enyo* displayed moderate and relatively uniform PLA_2 activity (mean 2.60; range 1.1–4.0; SD = 0.9). *Crotalus pyrrhus* showed generally low to moderate values (mean 1.96; range 0.5–4.1; SD = 1.2), although several individuals on Isla El Muerto (3.3–3.4), Isla Piojo (3.6), and the San Felipe mainland site (4.1) exhibited notably higher activity. *Crotalus ruber* showed the lowest and most uniform PLA_2 activity of all species (mean 1.95; range 0.2–3.2; SD = 0.7; Table 1). Ontogenetic regressions of PLA_2 activity against SVL revealed no significant relationships in any species ($p > 0.05$; Supplementary Table S4).

3.3. Proteolytic activity

Proteolytic activity differed significantly among species (Kruskal–Wallis: H = 39.28, df = 3, P < 0.001). Pairwise tests showed that *C. mitchellii* exhibited significantly lower activity than all other taxa (all $p_{adj} \leq 0.018$). Similarly, *C. enyo* demonstrated significantly lower activity compared to *C. pyrrhus* and *C. ruber* (both $p_{adj} \leq 0.044$), while the latter two species did not differ significantly from each other ($p_{adj} > 0.05$; Fig. 2; Supplementary Table S2). *Crotalus enyo* exhibited moderate proteolysis (mean 2.60; range 1.3–3.9; SD = 0.9), and *C. mitchellii* displayed uniformly low proteolysis (mean 0.35; range 0.13–1.44; SD = 0.4). *Crotalus pyrrhus* showed intermediate and relatively consistent activity (mean 3.97; range 2.4–5.1; SD = 0.8) across island and mainland localities. *Crotalus ruber* exhibited the highest proteolytic activity

Table 1
Biochemical activities and lethality of venoms. Individual values are shown; confidence intervals and ranges are provided in Supplementary Table S3. Mainland localities are denoted with roman numerals. BC = Baja California; BCS = Baja California Sur; I. = Isla (Fig. 1).

Locality	SVL (cm)	Venom complexity (*H*)	LD_{50} (μg/g)	PLA_2 activity (UAbs 405 nm)	Proteolytic activity (U/mg)	Proteolytic + EDTA (U/mg)	Fibrinogenolytic activity		
							Venom (α/β)	EDTA 5 mM (α/β)	PMSF 5 mM (α/β)
Crotalus enyo (n = 17)									
BC (II)	62.0	2.51	1.6	4.0	2.26	0.00	α	α^a	α
BCS (III)	58.0	2.52	ND	1.9	2.07	0.00	α, β^a	α^a, β^a	α
BCS (IV)	52.0	2.41	1.3	2.4	1.40	0.00	α	β^a	α
BCS (IV)	51.0	2.39	ND	2.3	1.42	0.00	α	β^a	α
BCS (IV)	59.5	2.51	0.72	2.9	2.89	0.00	α, β^a	β^a	α, β^a
BCS (V)	59.0	2.52	ND	1.9	1.90	1.40	α	α^a	α
BCS (V)	59.5	2.56	ND	2.3	2.10	0.00	α, β^a	β^a	α
BCS (VI)	60.0	2.41	ND	1.7	3.00	0.00	α^a, β^a	α^a	α, β
BCS (VI)	75.0	2.48	ND	4.0	3.04	0.00	α	α^a	α^a
I. Cerralvo	62.0	2.39	0.91	3.6	3.44	0.04	α	α^a	α^a
I. Cerralvo	63.5	2.44	1.25	1.8	3.25	0.00	α	α^a	α^a
I. Cerralvo	70.0	2.44	1.00	2.1	3.39	1.46	α	α^a	α^a
I. Esp. Santo	52.7	2.31	1.25	2.9	1.29	0.26	α	α^a	α
I. Partida Sur	51.1	2.39	1.60	1.1	3.26	1.49	α	α^a	α
I. San Fran.	47.1	2.43	0.72	3.7	3.71	0.00	α, β	β^a	α^a
I. San Fran.	52.7	2.52	2.20	1.9	1.95	0.00	α	α^a	α
I. San Jose	52.5	2.34	1.20	3.7	3.90	0.03	α, β^a	α^a, β^a	α^a
Crotalus mitchellii (n = 10)									
BCS (IV)	62.0	2.41	0.094	5.9	0.23	0.04	α^a, β^a	U	α^a
BCS (V)	73.0	2.19	ND	6.9	0.13	0.05	α^a, β^a	U	α, β
BCS (VI)	79.0	2.25	ND	5.9	0.19	0.10	α^a, β^a	α^a	α^a
I. Cerralvo	78.0	1.99	0.099	4.7	0.14	0.00	α	U	α^a
I. Cerralvo	78.0	2.15	0.12	5.3	0.14	0.03	α^a, β^a	U	α^a
I. Esp. Santo	62.0	2.07	0.098	6.1	0.34	0.28	α, β^a	U	α^a
I. Esp. Santo	63.0	1.84	0.07	6.1	0.14	0.00	α^a, β^a	β^a	α^a
I. Partida Sur	55.2	1.91	0.073	7.8	0.33	0.09	α^a	U	α^a
I. San Jose	60.5	2.09	0.080	5.6	1.44	0.42	α, β	U	α^a
I. San Jose	66.5	2.07	0.13	4.5	0.45	0.13	α, β^a	α, β	α^a
Crotalus pyrrhus (n = 14)									
BC (I)	74.5	1.86	1.70	4.1	5.10	0.03	α, β	β	α, β
BC (I)	51.5	2.30	ND	0.6	4.50	0.13	α, β	β	α, β
BC (II)	53.6	2.63	ND	1.5	4.60	0.03	α, β	β	α, β^a
I. Ang. Guard	115.0	1.81	2.20	0.9	4.50	0.17	α, β^a	U	α, β
I. Ang. Guard	119.0	1.85	2.20	1.4	4.80	0.21	α, β	β^a	α, β
I. Cabeza	45.5	2.64	3.30	2.1	3.20	0.08	α, β	α, β	α, β
I. Cabeza	55.5	2.41	3.30	2.0	2.40	0.08	α, β	β	α, β
I. Cabeza	71.0	1.80	3.70	0.5	4.67	0.04	α, β	α^a, β^a	α, β
I. El Muerto	53.4	2.48	0.72	3.4	3.90	0.09	α, β	β	α, β^a
I. El Muerto	61.0	2.50	0.86	3.3	4.39	0.60	α, β	α^a, β	α, β
I. Piojo	61.5	2.51	ND	3.6	3.76	0.63	α, β	α^a, β	α
I. Piojo	68.3	2.18	2.57	0.7	2.62	0.29	α, β	β	α
I. Smiths	55.6	2.64	0.90	1.2	3.23	0.65	α, β	α^a, β	α, β^a
I. Smiths	75.0	2.50	1.40	2.1	3.84	0.15	α, β	β	α^a, β^a
Crotalus ruber (n = 14)									
BC (I)	79.0	1.91	ND	1.7	5.80	0.06	ND	ND	ND
BC (II)	51.0	2.22	ND	1.5	1.20	0.13	α, β	β	α
BC (II)	66.5	2.08	ND	0.2	4.70	0.22	α, β	β	α, β
BCS (III)	91.0	1.77	3.00	1.8	5.46	0.00	α, β	β	α, β
BCS (IV)	95.5	1.65	ND	2.0	5.10	0.03	α, β	β	α, β
BCS (IV)	75.5	2.15	ND	1.9	6.48	0.00	α, β	β	α, β
BCS (IV)	82.0	1.95	2.60	1.8	5.52	0.05	α, β	β	α, β
BCS (V)	82.0	2.10	ND	2.6	6.76	0.00	α, β	β	α, β
BCS (V)	77.0	2.26	ND	3.2	3.30	0.10	α, β	β	α
BCS (V)	94.0	1.80	4.90	2.0	6.10	0.00	α, β	β	α, β
BCS (VI)	105.0	1.74	ND	2.4	8.04	0.00	α, β	β	α, β
I. Danzante	74.5	2.29	2.20	2.5	5.18	0.00	α, β	β	α, β
I. San Jose	73.5	2.18	2.10	1.9	5.78	0.00	α, β	β	α, β
I. San Jose	83.0	1.99	2.20	1.8	7.78	0.00	α, β	β	α, β

ND = not determined. U (Undegraded) indicates no detectable fibrinogen chain degradation.
[a] Indicates partial degradation.

(mean 5.51; range 1.2–8.0; SD = 1.7), with nearly all individuals between 5–8 U/mg, except for two mainland individuals from Baja II (1.20) and BCS V (3.3) with reduced activities (Table 1). A significant positive relationship between SVL and total proteolytic activity was found in *C. ruber* (R^2 = 0.50, p = 0.005), but not *C. enyo*, *C. mitchellii*, or *C. pyrrhus* (all $p > 0.05$; Supplementary Table S4).

3.4. Proteolytic activity post-EDTA exposure

EDTA-insensitive proteolytic activity was highly zero-inflated and varied significantly among species (Kruskal–Wallis: H = 12.51, df = 3, P = 0.005). Pairwise Dunn tests showed that *C. pyrrhus* had significantly higher EDTA-insensitive activity than both *C. enyo* and *C. ruber* (both

p_{adj} = 0.008), reflecting the consistently non-zero distribution in *C. pyrrhus* relative to the predominantly zero-inflated profiles of these congeners; all other pairwise comparisons were non-significant (p_{adj} > 0.05; Fig. 2; Supplementary Table S2). *Crotalus enyo* exhibited the greatest variance (mean 0.27; range 0.00–1.49; SD = 0.6), with most individuals showing no detectable EDTA-insensitive activity, but several producing high values, including individuals from Isla Partida Sur (1.49), Isla Cerralvo (1.46), BCS V (1.4), and Isla Espíritu Santo (0.26). *Crotalus pyrrhus* (mean 0.22; range 0.03–0.65; SD = 0.2) displayed elevated EDTA-insensitive activity on several islands, particularly Isla Smiths (0.65) and Isla Piojo (0.63), whereas populations on Isla Ángel de la Guarda and Isla Cabeza de Caballo were near zero. *C. mitchellii* (mean 0.11; range 0.00–0.42; SD = 0.1) remained uniformly low, and *C. ruber* (mean 0.04; range 0.00–0.22; SD = 0.1) exhibited almost exclusively near-zero activity across all sites (Table 1). A significant negative relationship between SVL and EDTA-insensitive proteolytic activity was only detected in *C. ruber* (R^2 = 0.35, p = 0.026; all other species $p > 0.05$; Supplementary Table S4).

3.5. Fibrinogenolytic activity

All individuals from all four species cleaved the α-chain of fibrinogen; however, the ability to hydrolyze the β-chain varied among taxa. In *C. enyo*, 6/17 venoms degraded the β-chain (including partial degradation, β^*), whereas 8/10 *C. mitchellii* venoms cleaved the β-chain. In contrast, all *C. pyrrhus* (14/14) and *C. ruber* (13/13) venoms hydrolyzed the β-chain. Thus, β-chain degradation was incomplete and variable in *C. enyo* and *C. mitchellii*, but uniformly present in *C. pyrrhus* and *C. ruber*. Pre-incubation with the SVMP inhibitor EDTA and the SVSP inhibitor PMSF altered fibrinogen cleavage patterns in a species-specific manner. In *C. mitchellii*, only 3/10 venoms retained any detectable cleavage following EDTA treatment, with the majority (7/10) yielding a complete Undegraded profile; in *C. ruber*, EDTA consistently eliminated α-chain cleavage while β-chain degradation persisted across all individuals (13/13). In *C. pyrrhus*, β-chain degradation persisted following EDTA treatment in nearly all individuals (13/14), and residual α-chain cleavage was also retained in 5/14 individuals. In *C. enyo*, residual α-chain cleavage (α^*) was retained in 12/17 individuals, while partial β-chain degradation (β^*) persisted in 7/17. Following PMSF treatment, β-chain cleavage persisted in only 2/17 *C. enyo* and 1/10 *C. mitchellii* individuals; in contrast, β-chain cleavage was retained in 11/13 *C. ruber* and 12/14 *C. pyrrhus* individuals despite PMSF inhibition (Table 1; Supplementary Figures S5–S34).

3.6. Venom lethality (LD_{50})

LD_{50} differed significantly among species (Kruskal–Wallis: H = 23.14, df = 3, P < 0.0001). Pairwise comparisons confirmed that *C. mitchellii* was significantly more potent than all other species (all $p_{adj} \leq 0.010$); *C. enyo* was also significantly more potent than *C. ruber* (p_{adj} = 0.040); all other pairwise comparisons were non-significant (p_{adj} > 0.05; Fig. 2; Supplementary Table S2). *C. mitchellii* possessed uniformly potent venom (mean LD_{50} 0.096; range 0.07–0.13; SD = 0.02), with minimal variation across islands. The primary cause of mortality was consistent with a neurotoxic mechanism, characterized by initial paralysis of the hind limbs followed by pronounced lateral muscle contractions, likely compensatory to progressive loss of diaphragmatic function, as described for crotoxin-mediated envenomation typical of a Type II (Type A) venom (Mackessy, 2010; Massey et al., 2012; Harris and Scott-Davey, 2013; Franco-Servín et al., 2021). *Crotalus enyo* exhibited moderate LD_{50} values (mean 1.25; range 0.72–2.2; SD = 0.44), with higher variance on Isla San Francisco (range 0.72–2.20; SD = 1.0). *C. pyrrhus* displayed the broadest range (mean 1.87; range 0.26–3.70; SD = 1.17), and LD_{50} was particularly low on Isla Piojo (0.26) and high on Isla Cabeza de Caballo (3.3–3.7). *C. ruber* exhibited the least potent venom (mean 2.83; range 2.1–4.9; SD = 1.1), with the highest LD_{50} observed across all samples (4.90 in BCS V; Table 1). SVL significantly and positively predicted LD_{50} only in *C. ruber* (R^2 = 0.68, p = 0.044; all other species $p > 0.05$; Supplementary Table S4).

3.7. Neutralization of lethal activity

Antivenom efficacy differed significantly among species for both metrics assessed: the mass of antivenom required to neutralize 1 mg of venom (mgAV/mgV; Kruskal–Wallis: H = 14.95, df = 3, P = 0.002) and the number of LD_{50} equivalents neutralized per vial (Kruskal–Wallis: H = 12.45, df = 3, P = 0.006; Fig. 3). For mgAV/mgV, pairwise Dunn tests showed that *C. mitchellii* required significantly more antivenom per mg venom than *C. enyo* (p_{adj} = 0.003) and *C. pyrrhus* (p_{adj} = 0.012); all other pairwise comparisons were non-significant (p_{adj} > 0.05; Supplementary Table S2). For LD_{50} equivalents per vial, only *C. mitchellii* versus *C. pyrrhus* (p_{adj} = 0.011) and *C. mitchellii* versus *C. ruber* (p_{adj} = 0.026) were significant; all other comparisons were non-significant (p_{adj} > 0.05; Supplementary Table S2).

When evaluated using mgAV/mgV, *C. mitchellii* required more antivenom per unit venom than any other species. Values ranged from 22.0 to 56.7 mgAV/mgV across island populations, indicating consistently reduced neutralization efficiency. In contrast, *C. enyo* venoms were neutralized efficiently, with low mgAV/mgV values across both island and a mainland sample (5.8–9.6 mgAV/mgV). *C. pyrrhus* exhibited intermediate and more variable antivenom requirements, with intermediate values on Isla El Muerto (7.0–11.0 mgAV/mgV) and Isla Smiths (10.0–11.0 mgAV/mgV) and higher values on Isla Cabeza de Caballo (11.3–17.2 mgAV/mgV) and Isla Ángel de la Guarda (12.1–20.0 mgAV/mgV). *C. ruber* also showed pronounced locality-level variation, with relatively low antivenom requirements on Isla San José (7.5 mgAV/mgV) but substantially higher values on Isla Danzante (21.5 mgAV/mgV).

Neutralization capacity (LD_{50}-equivalents per vial), evaluated against the manufacturer-stated reference of 790 LD_{50}s/vial for *C. durissus*, differed substantially among species. *Crotalus mitchellii* showed the highest values (565–2349 LD_{50}s/vial), with values spanning both below and above the reference threshold depending on locality. All tested *C. enyo* (339–630 LD_{50}s/vial) and *C. ruber* (84–240 LD_{50}s/vial) individuals fell below the reference, as did the majority of *C. pyrrhus* individuals; the greatest range was observed in *C. pyrrhus*, from very low values on Isla Cabeza de Caballo (72–109 LD_{50}s/vial) to values approaching or marginally exceeding the reference on Isla El Muerto (434–805 LD_{50}s/vial). Regressions of antivenom neutralization metrics against SVL revealed no significant relationships in *C. enyo*, *C. mitchellii*, or *C. pyrrhus* (all $p > 0.05$); *C. ruber* could not be assessed due to insufficient sample size (n = 2; Supplementary Table S4).

4. Discussion

The four rattlesnake species sampled across the Baja California Peninsula and Gulf of California islands exhibited functionally distinct venom phenotypes that spanned the Type I–Type II continuum, from the highly neurotoxic profile of *C. mitchellii* to the metalloprotease-dominated phenotypes of *C. pyrrhus* and *C. ruber*. Such functional diversity builds on previously documented compositional variation in this system (Glenn and Straight, 1985; Arnaud-Franco et al., 2018; Rodríguez-Canseco et al., 2021; Arnaud-Franco et al., 2023; Hirst et al., 2024, 2025, 2026) and demonstrates that protein expression differences translate into meaningful divergence in enzymatic activity, lethality, and antivenom neutralization for these species. Although restricted per-locality sample sizes precluded formal tests of intra-specific geographic variation, these species-level contrasts establish a framework for understanding functional divergence in this region and its biomedical consequences (Table 1).

Crotalus mitchellii exhibited a venom phenotype characterized by elevated PLA_2 activity and extreme potency in murine lethality assays, consistent with a Type II venom (Glenn et al., 1983; Glenn and Straight, 1985; Mackessy, 2010; Harris and Scott-Davey, 2013; Mackessy, 2021). The combination of significantly higher PLA_2 activity and lower LD_{50}

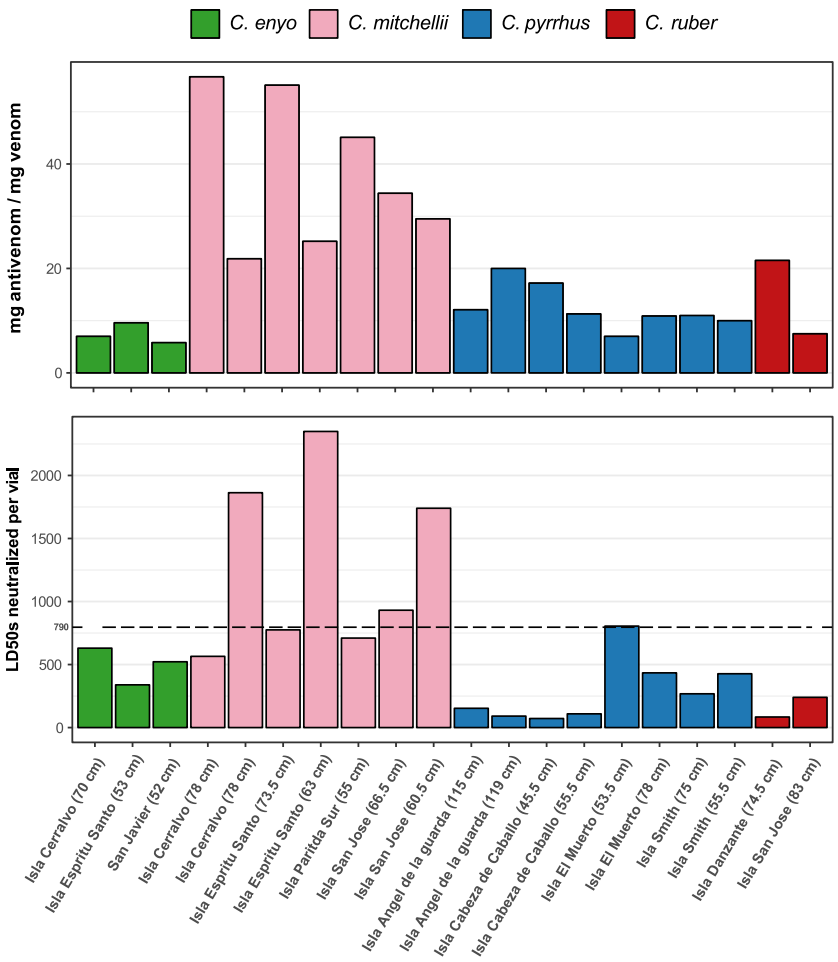

Fig. 3. Antivenom neutralization efficiency across Baja California rattlesnake species from island and mainland localities. The top panel shows antivenom requirement expressed as mg antivenom per mg venom (mgAV/mgV), and the bottom panel shows the number of LD_{50} doses neutralized per vial of antivenom. Horizontal dotted line indicates the reference neutralization capacity of 790 LD_{50} doses per vial, established for *Crotalus durissus* venom by Antivipmyn®. Bars are colored by species. Locality names and snout–vent length (SVL) are indicated along the *x*-axis. (For interpretation of the references to color in this figure legend, the reader is referred to the web version of this article.)

relative to all three congeners is consistent with the presence of potent presynaptic neurotoxic complexes, such as Mojave toxin, which dominate the venom functional phenotype of this lineage (Glenn et al., 1983; Glenn and Straight, 1985; Harris and Scott-Davey, 2013). Interestingly, despite having the lowest overall proteolytic activity among the sampled taxa, *C. mitchellii* retained the ability to degrade fibrinogen. Ubiquitous α-chain cleavage and prevalent β-chain degradation are characteristic of other Type II/A rattlesnake venoms, where a basal set of proteases is maintained despite reduced expression (Mackessy, 2010; Calvete et al., 2012). EDTA abolished detectable fibrinogen degradation in most individuals, implicating SVMPs as the primary contributors to this residual fibrinogenolytic activity (Estêvão-Costa et al., 2000; Swenson and Markland, 2005). However, the contribution of SVMPs to fibrinogen degradation should be interpreted with caution in a clinical context. *In vivo*, SVMPs are generally thought to act predominantly at the envenomation site, targeting extracellular matrix components and thereby limiting systemic effects (Gutiérrez and Rucavado, 2000; Gutiérrez et al., 2016). Consequently, their role in circulating fibrinogen degradation in envenomed patients may be relatively minor (Kini and Koh, 2016). In contrast, the neurotoxic components of Type II venoms are expected to drive the primary clinical manifestations (Gutiérrez et al., 2017; Mackessy, 2021). A minority of individuals retained partial cleavage following EDTA treatment, suggesting that some EDTA-resistant, non-SVMP fibrinogenolytic activity persists in this species. PMSF treatment typically reduced cleavage to partial α degradation with diminished β cleavage, indicating variable or secondary contributions from SVSPs (Shimokawa et al., 1996; Roldán-Padrón et al., 2019). Low venom complexity of *C. mitchellii* also aligned with the dominance of PLA_2-based neurotoxic components in the species, effectively reducing the relative contribution of other toxin families (Mackessy, 2010; Calvete et al., 2012; Mackessy, 2021; Margres et al., 2021). Antivenom assays further highlighted the clinical trade-offs of this phenotype. Although *C. mitchellii* venom required a substantially higher antibody mass (mgAV/mgV) for neutralization, the extreme potency of the venom means a single vial can neutralize a large number of LD_{50} equivalents (Secretaría de Salud, 2012; Guadarrama-Martínez et al., 2024). Together, these results delineate a specialized, highly potent venom that favors neurotoxicity over tissue degradation characteristic of more proteolytic-dominant venoms (Mackessy, 2010, 2021). Despite this species-level functional homogeneity, modest locality-level variation was apparent: proteolytic activity was locally elevated on Isla San José relative to other sampled populations, indicating localized SVMP activity that contrasts with the otherwise suppressed proteolytic profile characteristic of this species, whereas LD_{50} remained strikingly consistent across all localities sampled, indicating that the potency of the neurotoxic phenotype is largely conserved geographically despite documented compositional variation among assemblage populations (Hirst et al., 2025). Clinically, envenomation by *C. mitchellii* would be expected to present primarily as systemic neurotoxicity rather than local tissue damage, and although antivenom dosing requires greater

antibody mass, the high potency-scaled neutralization suggests that timely administration of Antivipmyn® remains a viable treatment strategy.

C. pyrrhus exhibited a proteolytic-dominant, Type I venom phenotype (Glenn and Straight, 1985; Mackessy, 2010; Rokyta et al., 2013; Borja et al., 2014; Mackessy, 2021), contrasting sharply with the neurotoxic activities of its sister taxon, *C. mitchellii* (Holding et al., 2021; Farleigh et al., 2026). Total proteolysis was consistently high, and fibrinogenolytic activity was not only ubiquitous, but broad in scope. All individuals degraded both α- and β-chains, indicating stable expression of enzymes capable of comprehensive fibrinogen hydrolysis (Swenson and Markland, 2005). The inhibitor profile of *C. pyrrhus* was particularly distinctive. β-chain degradation persisted following EDTA treatment in nearly all individuals, indicating a substantial contribution from EDTA-resistant SVSPs that was less pronounced in its congeners (Shimokawa et al., 1996; Roldán-Padrón et al., 2019). Meanwhile, cleavage activity largely persisted following PMSF treatment, with both chains remaining degraded in most individuals, reinforcing the interpretation of a high overall proteolytic load with mixed contributions of SVMPs and SVSPs (Shimokawa et al., 1996; Terra et al., 2009). This mixed SVMP/SVSP strategy, coupled with low PLA_2 activity and higher (less potent) lethality values than *C. mitchellii*, defines a coagulopathic predatory strategy in which divergent toxin classes synergistically disrupt host hemostasis (Mackessy, 1988, 2010, 2021). Neutralization assays further distinguished the two sister taxa: *C. pyrrhus* required moderate but variable mgAV/mgV ratios compared to the substantially higher antibody mass requirements of *C. mitchellii*, with pronounced locality-level variation, ranging from comparatively low requirements on Isla El Muerto and Isla Smiths to substantially higher values on Isla Cabeza de Caballo and Isla Ángel de la Guarda. This geographic gradient in antivenom requirements parallels locality-level patterns in both lethality and enzymatic activity: LD_{50} was lowest on Isla El Muerto and highest on Isla Cabeza de Caballo, while EDTA-insensitive proteolytic activity was elevated on Isla Smiths and Isla Piojo but near zero on Isla Ángel de la Guarda and Isla Cabeza de Caballo (Table 1). Together, these patterns suggest that functional activities in *C. pyrrhus* venom diverge across insular localities. Additionally, *C. pyrrhus* displayed high among-individual variation in complexity across insular and mainland localities (Hirst et al., 2025), which mirrors the broad functional variability documented here. From a clinical perspective, envenomation by *C. pyrrhus* would be expected to present as coagulopathy and hemostatic disruption (Cochran et al., 2019), and the pronounced locality-level variation in antivenom requirements underscores the importance of monitoring neutralization response in patients bitten across different populations.

Crotalus ruber also exhibited a proteolytic-dominant phenotype consistent with a Type I venom profile (Glenn and Straight, 1985; Mackessy, 2010, 2021). This species showed the highest total proteolytic activity among the studied taxa, though not significantly different from *C. pyrrhus* ($p_{adj} = 0.070$), and uniformly degraded both α- and β-chains of fibrinogen across all individuals. This dual-chain degradation pattern was maintained consistently across insular (Isla Danzante, Isla San José) and all mainland localities sampled (BC I through BCS VI), suggesting a geographically canalized proteolytic phenotype in *C. ruber* despite prior documentation of compositional variation across its range (Hirst et al., 2024). Although it shared this uniform cleavage pattern with *C. pyrrhus*, the inhibitor profiles revealed distinct biochemical activities. EDTA treatment consistently eliminated α-chain degradation while β-chain cleavage persisted across all individuals, indicating that α-cleavage is predominantly SVMP-mediated, whereas β-chain degradation involves EDTA-resistant proteases such as SVSPs (Shimokawa et al., 1996; Roldán-Padrón et al., 2019). This contrasts with *C. pyrrhus*, where both chains frequently persisted under EDTA, suggesting a broader SVSP contribution to fibrinogenolysis in that species. PMSF treatment rarely eliminated degradation in *C. ruber*, with both chains persisting in the majority of individuals, indicating that SVMPs carry the dominant proteolytic load overall despite the SVSP contribution to β-cleavage specifically. The reliance on SVMPs likely drives tissue destruction and local edema characteristic of *C. ruber* envenomation (Glenn and Straight, 1985; Straight et al., 1992; Pozas-Ocampo et al., 2020). *C. ruber* showed the lowest overall complexity, consistent with its functional specialization toward SVMP-dominated proteolysis. The repeated detection of significant SVL relationships across proteolytic activity, lethality, and venom complexity demonstrates a continuous ontogenetic shift in the functional venom phenotype in *C. ruber*, revealing that the continuous compositional shifts translate directly into functional consequences (Hirst et al., 2024). Such pattern was recovered despite all sampled individuals exceeding 51 cm SVL, demonstrating that ontogenetic functional divergence persists beyond a discrete juvenile–adult transition. Geographic and ontogenetic factors should therefore be considered when interpreting individual-level functional variation in this species. In neutralization assays, the two *C. ruber* individuals yielded divergent results, with the individual from Isla San José requiring substantially less antivenom per mg venom than the individual from Isla Danzante, among the lowest values recorded for any non-neurotoxic species tested here. Such divergence is notable given the otherwise highly uniform proteolytic functional profile of this species across localities. Furthermore, LD_{50} equivalents neutralized per vial were among the lowest of any species tested, a result consistent with the reduced venom potency of *C. ruber* relative to the other taxa. The functional signature of *C. ruber* venom thus aligns with SVMP-rich, hemorrhagic Type I/B venoms that emphasize tissue destruction and systemic hemostatic disruption (Estêvão-Costa et al., 2000; Bernardoni et al., 2014; Yamashita et al., 2014; Kini and Koh, 2016). Envenomation by *C. ruber* would accordingly be expected to present as local tissue destruction and hemorrhage (Lyons, 1971); however, these clinical effects were not directly evaluated in the present study. Additionally, the limited and variable antivenom data available for this species across its geographic range, including island populations, highlight the need for expanded sampling to establish reliable neutralization benchmarks.

Crotalus enyo exhibited an intermediate and notably variable functional profile. Moderate PLA_2 activity, proteolysis, and lethality placed the species between the neurotoxic extreme of Type II *C. mitchellii* and the highly proteolytic phenotypes of Type I *C. pyrrhus* and *C. ruber* (Mackessy, 2010). This taxon was also characterized by notable intraspecific variation in fibrinogenolytic patterns. Although α-cleavage was universal, only a minority of individuals (6/17) exhibited β-chain degradation. Among those individuals displaying β-degradation, activity generally persisted following EDTA treatment but was abolished by PMSF, suggesting that β-cleavage in *C. enyo* is primarily mediated by SVSPs in the subset of individuals where it occurs (Swenson and Markland, 2005). Although a similar SVSP contribution to β-cleavage was observed in *C. ruber*, this activity was uniformly expressed in that species but remained inconsistent and individual-specific in *C. enyo*. Similarly, EDTA-insensitive proteolytic activity was elevated at a subset of localities, including Isla Partida Sur, Isla Cerralvo, Isla Espíritu Santo, and one individual from the BCS V mainland site, while all remaining individuals yielded near-zero activity (Table 1). The geographic clustering of this SVSP-mediated function across specific island and mainland populations suggests that SVSP expression in *C. enyo* is not uniformly distributed across its range, and may reflect population-level variation in venom composition consistent with compositional divergence previously documented between populations of this species (Hirst et al., 2026). *Crotalus enyo* venom also exhibited the highest and most uniform complexity, reflecting the maintenance of a broad enzymatic repertoire across toxin families. Despite its intermediate enzymatic profile, *C. enyo* was the most efficiently neutralized species, requiring the lowest mgAV/mgV values of the four taxa. Combined with moderate lethality, this resulted in favorable potency-scaled neutralization (LD_{50} equivalents per vial). This dissociation between intermediate functional activity and high neutralization efficiency suggests that the functional venom phenotype of *C. enyo*, while diverse, presents antigenic targets

that are highly congruent with the Antivipmyn® antibody pool. The favorable neutralization profile of *C. enyo* suggests that Antivipmyn® is well suited for managing envenomation by this species across its range, despite the functional variability observed among individuals.

Across all four species, the degree to which functional venom activity varied at the locality level differed substantially. *Crotalus mitchellii* and *C. ruber* exhibited comparatively consistent functional phenotypes across their sampled geographic ranges, particularly in the traits most diagnostic of their respective venom strategies (lethality for *C. mitchellii*; proteolytic profile for *C. ruber*), suggesting that species-level venom identity is largely conserved despite geographic differentiation across the peninsula and islands sampled here. In contrast, *C. pyrrhus* and *C. enyo* displayed more spatially structured functional variation, with lethality, antivenom requirements, and SVSP-mediated activities each showing clear locality-level differences across islands and mainland sites.

The results of this study also underscore broader challenges associated with antivenom treatment in Mexico. Polyvalent antivenoms must provide coverage across approximately 74 viper species (Guadarrama-Martínez et al., 2024), many of which show substantial ontogenetic and geographic variation in venom composition and function (Durban et al., 2017; Borja et al., 2018; Neri-Castro et al., 2019; Colis-Torres et al., 2022; Neri-Castro et al., 2022; Hirst et al., 2025; Borja et al., 2025). Although Antivipmyn® neutralized the lethal activity of all four venoms, the number of LD_{50} equivalents neutralized per vial was considerably lower for the less potent species. The limited samples available for *C. enyo* ($n = 3$) and *C. ruber* ($n = 2$) all fell below the manufacturer-stated reference of 790 LD_{50}-equivalents per vial for *C. durissus*, as did most *C. pyrrhus* individuals tested; *C. mitchellii* showed the opposite pattern, frequently exceeding the reference given its extreme venom potency. Such outcome is partly a consequence of the metric itself: species with less potent venom require a greater mass to constitute a lethal dose, and therefore more antibodies to neutralize each LD_{50} equivalent, reducing the count per vial regardless of per-venom neutralization efficiency (Minton and Weinstein, 1986; Fry et al., 2003; Massey et al., 2012; Borja et al., 2025). Although this does not necessarily indicate poor clinical performance of Antivipmyn®, it emphasizes the importance of dose optimization and clinical monitoring, particularly in insular settings, where limited access to medical care and delayed treatment times further compound the challenges of managing envenomation (Warrell, 2010; Rangel-Camacho et al., 2025).

Finally, it must be acknowledged that the statistical results involving neutralization assays and associated species-level comparisons should be interpreted with caution. The limited sample sizes available for several taxa in the neutralization assays (*C. enyo*: $n = 3$; *C. ruber*: $n = 2$) restricted the statistical power to detect significant differences, highlighting the necessity for expanded sampling to fully resolve antivenom neutralization of these rattlesnake venoms.

Our results demonstrate that the four focal rattlesnake species possess functionally distinct venom phenotypes spanning the Type I–Type II continuum, with differences carrying both ecological (Hirst et al., 2025, 2026) and biomedical implications. Although Antivipmyn® effectively neutralized all four venoms, neutralization efficiency varied significantly among taxa, underscoring that functional venom phenotype can predict antivenom performance and that species-level identification remains critical for clinical management in a region with frequent human-rattlesnake encounters (Bolon et al., 2020; Schmitz and Diaz, 2013; Olmos-Martínez et al., 2018; Grismer, 2002). Determining whether previously documented population-level differences in venom expression (Hirst et al., 2024, 2025, 2026) translate into clinically or ecologically meaningful functional divergence will require expanded geographic sampling and prey-specific functional assays. Nonetheless, this study establishes that among-species venom variation in rattlesnakes across the Baja California Peninsula and Gulf of California islands extends beyond protein expression to encompass functional activity and antivenom neutralization.

CRediT authorship contribution statement

Samuel R. Hirst: Writing – original draft, Investigation, Funding acquisition, Formal analysis, Data curation, Conceptualization. **Edgar Neri-Castro:** Writing – original draft, Supervision, Investigation, Funding acquisition, Formal analysis, Data curation, Conceptualization. **Emiliano Vázquez-García:** Investigation. **Vanessa Zarzosa:** Investigation. **Felipe Olvera:** Investigation. **Cameron M. VanHorn:** Investigation. **Alejandro Alagón:** Investigation. **Hector Franz-Chávez:** Investigation. **Gamaliel Castañeda-Gaytán:** Investigation. **Christopher L. Parkinson:** Investigation. **Jason L. Strickland:** Investigation. **Miguel Borja:** Investigation. **Mark J. Margres:** Writing – review & editing, Supervision, Investigation, Funding acquisition, Conceptualization.

Ethical statement

Sampling was conducted under permits issued by the Secretaría de Medio Ambiente y Recursos Naturales (SGPA/DGVS: 06166/20, 01178/20, 04856/21, 04999/22). All procedures followed ethical guidelines approved by the Institutional Animal Care and Use Committees (IACUC) at the University of South Florida (protocol IS00011949) and Clemson University (protocol 2017- 067). Animal use was approved by the bioethics committee of the Institute of Biotechnology at UNAM, project #471.

Funding

This work was supported by, the National Science Foundation Graduate Research Fellowship Program grant no. 2136515 awarded to S.R.H, the National Geographic Society (NGS-91224R-21) awarded to M.J.M., J.L.S., M.B., G.C.-G., C.L.P., and H.F.-C., the American Museum of Natural History Theodore Roosevelt Memorial Fund awarded to M.J.M., the *Western North American Naturalist* Natural History Research Grant awarded to S.R.H, and the National Science Foundation (DEB 1638879 and DEB 1822417) awarded to C.L.P. We acknowledge support from the DGAPA-PAPIIT, UNAM project IA202826 ("Análisis genómico, transcriptómico *y* proteómico de toxinas, *y* caracterización funcional del veneno de Bothrops asper"), which provided reagents and resources that, although originally acquired for a different project, were also used in this study

Declaration of competing interest

The authors declare that they have no known competing financial interests or personal relationships that could have appeared to influence the work reported in this paper.

Acknowledgments

We would like to thank Víctor Vásquez-Cruz, Alfonso Kelly-Hernández, Alexandra Rubio Rincón, Tania Perez Fiol, David Emaús López Martínez, Sofía Alejandra Salinas Amézquita, Ramsés Alejandro Rosales-García, Chris Grünwald, Chris Rodriguez, Brandon La Forest, Jacobo Reyes-Valasquez, Brandon Deitrich, and Jacob Loyacano for their help with sampling. We thank Luz Aurora Hurtado, Irma Gonzalez, and Raol Preciado with CONANP and the Parque Nacional Archipiélago de Espíritu Santo, Jesus Oswaldo Amador Fernandez, Iris del Castillo Velasco Martínez, Yessica Mariana Salgado Gallegos, and Rodolfo Palacios Romo with CONANP and the Parque Nacional Bahía de Loreto, and María del Carmen Hernandez Ramírez and Rosalía Ávalos Téllez with the Zona Marina Bahía de los Ángeles for access to field sites. We would also like to thank Ricardo Smiths, Samberto Castro, and Alejandro Flores Rizo for transportation to the islands. Snake image credits: Ricardo Ramírez Chaparro and Jacob Loyacano.

Appendix A. Supplementary data

Supplementary material related to this article can be found online at https://doi.org/10.1016/j.toxicon.2026.109266.

Data availability

The data underlying this article are available in its online supplementary material. Metadata are provided in Supplementary Table S3. All analytical softwares are publicly available.

References

Alape-Girón, A., Sanz, L., Escolano, J., Flores-Díaz, M., Madrigal, M., Sasa, M., Calvete, J.J., 2008. Snake venomics of the lancehead pitviper bothrops asper: Geographic, individual, and ontogenetic variations. J. Proteome Res. 7 (8), 3556–3571. http://dx.doi.org/10.1021/pr800332p.

Andrade, D.V., Abe, A.S., 1999. Relationship of venom ontogeny and diet in bothrops. Herpetologica 55 (2), 200–204, arXiv:3893080.

Arnaud-Franco, G., Cordero-Tapia, A., Ortíz-Ávila, V., Moctezuma-González, C.L., Tejocote-Pérez, M., Carbajal-Saucedo, A., 2018. Comparison of biological and biochemical characteristics of venom from rattlesnakes in the southern Baja California Peninsula. Toxicon 148, 197–201. http://dx.doi.org/10.1016/j.toxicon.2018.04.030.

Arnaud-Franco, G., Ríos-Castro, E., Velasco-Suárez, A., García-de León, F.J., Beltrán, L.F., Carbajal-Saucedo, A., 2023. Venom comparisons of endemic and micro-endemic speckled rattlesnakes *Crotalus Mitchellii, C. Polisi and C. Thalassoporus* from Baja California Peninsula. Toxicon 224, 107030. http://dx.doi.org/10.1016/j.toxicon.2023.107030.

Barlow, A., Pook, C.E., Harrison, R.A., Wüster, W., 2009. Coevolution of diet and prey-specific venom activity supports the role of selection in snake venom evolution. Proc. R. Soc. B: Biological Sci. 276 (1666), 2443–2449. http://dx.doi.org/10.1098/rspb.2009.0048.

Bernardoni, J.L., Sousa, L.F., Wermelinger, L.S., Lopes, A.S., Prezoto, B.C., Serrano, S.M.T., Zingali, R.B., Moura-da-Silva, A.M., 2014. Functional variability of snake venom metalloproteinases: Adaptive advantages in targeting different prey and implications for human envenomation. PLoS One 9 (10), e109651. http://dx.doi.org/10.1371/journal.pone.0109651.

Bolon, I., Durso, A.M., Mesa, S.B., Ray, N., Alcoba, G., Chappuis, F., de Castañeda, R.R., 2020. Identifying the snake: First scoping review on practices of communities and healthcare providers confronted with snakebite across the world. PLoS One 15 (3), e0229989. http://dx.doi.org/10.1371/journal.pone.0229989.

Borja, M., Castañeda-Gaytán, G., Alagón, A., Strickland, J.L., Parkinson, C.L., Gutiérrez-Martínez, A., Rodriguez-López, B., Zarzosa, V., Lomonte, B., Saviola, A.J., Fernández, J., Smith, C.F., Hansen, K.C., Pérez-Robles, A., Castañeda-Pérez, S., Hirst, S.R., Olvera-Rodríguez, F., Fernández-Badillo, L., Sigala, J., Jones, J., Montaño-Ruvalcaba, C., Ramírez-Chaparro, R., Margres, M.J., Acosta-Campaña, G., Neri-Castro, E., 2025. Venom variation and ontogenetic changes in the *Crotalus Molossus* complex: Insights into composition, activities, and antivenom neutralization. Comp. Biochem. Physiol. C: Toxicol. Pharmacol. 290, 110129. http://dx.doi.org/10.1016/j.cbpc.2025.110129.

Borja, M., Castañeda, G., Espinosa, J., Neri, E., Carbajal, A., Clement, H., García, O., Alagon, A., 2014. Mojave rattlesnake (Crotalus Scutulatus Scutulatus) with Type B Venom from Mexico. Copeia 2014 (1), 7–13. http://dx.doi.org/10.1643/OT-12-041.

Borja, M., Neri-Castro, E., Pérez-Morales, R., Strickland, J.L., Ponce-López, R., Parkinson, C.L., Espinosa-Fematt, J., Sáenz-Mata, J., Flores-Martínez, E., Alagón, A., Castañeda-Gaytán, G., 2018. Ontogenetic change in the venom of mexican black-tailed rattlesnakes (Crotalus molossus nigrescens). Toxins 10 (12), 501. http://dx.doi.org/10.3390/toxins10120501.

Calvete, J.J., 2010. Antivenomics and venom phenotyping: A marriage of convenience to address the performance and range of clinical use of antivenoms. Toxicon 56 (7), 1284–1291. http://dx.doi.org/10.1016/j.toxicon.2009.12.015.

Calvete, J.J., Pérez, A., Lomonte, B., Sánchez, E.E., Sanz, L., 2012. Snake venomics of crotalus tigris: The minimalist toxin arsenal of the deadliest neartic rattlesnake venom. Evolutionary clues for generating a pan-specific antivenom against Crotalid Type II Venoms. J. Proteome Res. 11 (2), 1382–1390. http://dx.doi.org/10.1021/pr201021d.

Casasola, A., Ramos-Cerrillo, B., de Roodt, A.R., Saucedo, A.C., Chippaux, J.-P., Alagón, A., Stock, R.P., 2009. Paraspecific neutralization of the venom of African species of cobra by an equine antiserum against *Naja Melanoleuca*: A comparative study. Toxicon 53 (6), 602–608. http://dx.doi.org/10.1016/j.toxicon.2009.01.011.

Casewell, N.R., Jackson, T.N.W., Laustsen, A.H., Sunagar, K., 2020. Causes and Consequences of Snake Venom Variation. Trends Pharmacol. Sci. 41 (8), 570–581. http://dx.doi.org/10.1016/j.tips.2020.05.006.

Casewell, N.R., Wagstaff, S.C., Harrison, R.A., Renjifo, C., Wüster, W., 2011. Domain loss facilitates accelerated evolution and neofunctionalization of duplicate snake venom metalloproteinase toxin genes. Mol. Biol. Evol. 28 (9), 2637–2649. http://dx.doi.org/10.1093/molbev/msr091.

Casewell, N.R., Wagstaff, S.C., Wüster, W., Cook, D.A.N., Bolton, F.M.S., King, S.I., Pla, D., Sanz, L., Calvete, J.J., Harrison, R.A., 2014. Medically important differences in snake venom composition are dictated by distinct postgenomic mechanisms. Proc. Natl. Acad. Sci. 111 (25), 9205–9210. http://dx.doi.org/10.1073/pnas.1405484111.

Casewell, N.R., Wüster, W., Vonk, F.J., Harrison, R.A., Fry, B.G., 2013. Complex cocktails: The evolutionary novelty of venoms. Trends Ecol. Evolut. 28 (4), 219–229. http://dx.doi.org/10.1016/j.tree.2012.10.020.

Cipriani, V., Debono, J., Goldenberg, J., Jackson, T.N.W., Arbuckle, K., Dobson, J., Koludarov, I., Li, B., Hay, C., Dunstan, N., Allen, L., Hendrikx, I., Kwok, H.F., Fry, B.G., 2017. Correlation between ontogenetic dietary shifts and venom variation in Australian brown snakes (Pseudonaja). Comp. Biochem. Physiol. C: Toxicol. Pharmacol. 197, 53–60. http://dx.doi.org/10.1016/j.cbpc.2017.04.007.

Cochran, C., Hax, S., Hayes, W.K., 2019. Case reports of envenomation and venom composition differences between two Arizona populations of the Southwestern Speckled Rattlesnake, *Crotalus Pyrrhus* (Cope, 1867). Toxicon 171, 29–34. http://dx.doi.org/10.1016/j.toxicon.2019.09.022.

Colis-Torres, A., Neri-Castro, E., Strickland, J.L., Olvera-Rodríguez, A., Borja, M., Calvete, J., Jones, J., Parkinson, C.L., Bañuelos, J., López de León, J., Alagón, A., 2022. Intraspecific venom variation of Mexican West Coast Rattlesnakes (*Crotalus Basiliscus*) and its implications for antivenom production. Biochimie 192, 111–124. http://dx.doi.org/10.1016/j.biochi.2021.10.006.

Daltry, J.C., Wüster, W., Thorpe, R.S., 1996. Diet and snake venom evolution. Nature 379 (6565), 537–540. http://dx.doi.org/10.1038/379537a0.

Durban, J., Sanz, L., Trevisan-Silva, D., Neri-Castro, E., Alagón, A., Calvete, J.J., 2017. Integrated venomics and venom gland transcriptome analysis of juvenile and adult mexican rattlesnakes crotalus simus, C. tzabcan, and C. Culminatus revealed miRNA-modulated ontogenetic shifts. J. Proteome Res. 16 (9), 3370–3390. http://dx.doi.org/10.1021/acs.jproteome.7b00414.

Estêvão-Costa, M.I., Diniz, C.R., Magalhães, A., Markland, F.S., Sanchez, E.F., 2000. Action of Metalloproteinases Mutalysin I and II on several components of the hemostatic and fibrinolytic systems. Thromb. Res. 99 (4), 363–376. http://dx.doi.org/10.1016/S0049-3848(00)00259-0.

Farleigh, K., Highland, D.K., Alderman, M.G., Francioli, Y., Hirst, S.R., Faber, E.M., Perry, B.W., Holding, M.L., Castañeda-Gaytán, G., Borja, M., Franz-Chávez, H., Parkinson, C.L., Strickland, J.L., Margres, M.J., Mackessy, S.P., Meik, J.M., Castoe, T.A., Schield, D.R., 2026. Evolution of genome-wide barriers to gene flow during complex speciation in rattlesnakes. Proc. Natl. Acad. Sci. 123 (21), e2609058123. http://dx.doi.org/10.1073/pnas.2609058123.

Franco-Servín, C., Neri-Castro, E., Bénard-Valle, M., Alagón, A., Rosales-García, R.A., Guerrero-Alba, R., Poblano-Sánchez, J.E., Silva-Briano, M., Guerrero-Barrera, A.L., Sigala-Rodríguez, J.J., 2021. Biological and biochemical characterization of coronado island rattlesnake (Crotalus helleri caliginis) venom and antivenom neutralization. Toxins 13 (8), 582. http://dx.doi.org/10.3390/toxins13080582.

Fry, B.G., Winkel, K.D., Wickramaratna, J.C., Hodgson, W.C., Wüster, W., 2003. Effectiveness of snake antivenom: Species and regional venom variation and its clinical impact. J. Toxicol.: Toxin Rev. 22 (1), 23–34. http://dx.doi.org/10.1081/TXR-120019018.

Gené, J., Roy, A., Rojas, G., Gutiérrez, J., Cerdas, L., 1989. Comparative study on coagulant, defibrinating, fibrinolytic and fibrinogenolytic activities of Costa Rican crotaline snake venoms and their neutralization by a polyvalent antivenom. Toxicon 27 (8), 841–848. http://dx.doi.org/10.1016/0041-0101(89)90096-2.

Gibbs, H.L., Rossiter, W., 2008. Rapid evolution by positive selection and gene gain and loss: PLA2 venom genes in closely related sistrurus rattlesnakes with divergent diets. J. Mol. Evol. 66 (2), 151–166. http://dx.doi.org/10.1007/s00239-008-9067-7.

Glenn, J.L., Straight, R., 1978. Mojave rattlesnake Crotalus Scutulatus Scutulatus venom: Variation in toxicity with geographical origin. Toxicon 16 (1), 81–84. http://dx.doi.org/10.1016/0041-0101(78)90065-X.

Glenn, J.L., Straight, R.C., 1985. Venom properties of the rattlesnakes (*Crotalus*) inhabiting the Baja California region of Mexico. Toxicon 23 (5), 769–775. http://dx.doi.org/10.1016/0041-0101(85)90007-8.

Glenn, J.L., Straight, R.C., Wolfe, M.C., Hardy, D.L., 1983. Geographical variation in *Crotalus Scutulatus Scutulatus* (Mojave rattlesnake) venom properties. Toxicon 21 (1), 119–130. http://dx.doi.org/10.1016/0041-0101(83)90055-7.

Grismer, L.L., 2002. Amphibians and reptiles of Baja California, Including Its Pacific Islands and the Islands in the Sea of Cortés. University of California Press.

Guadarrama-Martínez, A., Neri-Castro, E., Boyer, L., Alagón, A., 2024. Variability in antivenom neutralization of Mexican viperid snake venoms. PLOS Neglected Trop. Dis. 18 (5), e0012152. http://dx.doi.org/10.1371/journal.pntd.0012152.

Gutiérrez, J.M., Calvete, J.J., Habib, A.G., Harrison, R.A., Williams, D.J., Warrell, D.A., 2017. Snakebite envenoming. Nat. Rev. Dis. Prim. 3 (1), 17063. http://dx.doi.org/10.1038/nrdp.2017.63.

Gutiérrez, J.M., Escalante, T., Rucavado, A., Herrera, C., Fox, J.W., 2016. A Comprehensive View of the Structural and Functional Alterations of Extracellular Matrix by Snake Venom Metalloproteinases (SVMPs): Novel Perspectives on the Pathophysiology of Envenoming. Toxins 8 (10), 304. http://dx.doi.org/10.3390/toxins8100304.

Gutiérrez, J.M., Rucavado, A., 2000. Snake venom metalloproteinases:Their role in the pathogenesis of local tissue damage. Biochimie 82 (9), 841–850. http://dx.doi.org/10.1016/S0300-9084(00)01163-9.

Gutiérrez, J.M., Sanz, L., Escolano, J., Fernández, J., Lomonte, B., Angulo, Y., Rucavado, A., Warrell, D.A., Calvete, J.J., 2008. Snake venomics of the lesser antillean pit vipers bothrops caribbaeus and bothrops lanceolatus: Correlation with toxicological activities and immunoreactivity of a heterologous antivenom. J. Proteome Res. 7 (10), 4396–4408. http://dx.doi.org/10.1021/pr8003826.

Harris, J.B., Scott-Davey, T., 2013. Secreted phospholipases A2 of snake venoms: Effects on the peripheral neuromuscular system with comments on the role of Phospholipases A2 in disorders of the CNS and their uses in industry. Toxins 5 (12), 2533–2571. http://dx.doi.org/10.3390/toxins5122533.

Hirst, S.R., Beer, M.A., VanHorn, C.M., Rautsaw, R.M., Franz-Chávez, H., Lopez, B.R., Chaparro, R.R., Rosales-García, R.A., Vásquez-Cruz, V., Kelly-Hernández, A., Amézquita, S.A.S., Martínez, D.E.L., Fiol, T.P., Rincón, A.R., Whittington, A.C., Castañeda-Gaytán, G., Borja, M., Parkinson, C.L., Strickland, J.L., Margres, M.J., 2025. Island biogeography and competition drive rapid venom complexity evolution across rattlesnakes. Evolution 79 (8), 1419–1432. http://dx.doi.org/10.1093/evolut/qpaf074.

Hirst, S.R., Rautsaw, R.M., VanHorn, C.M., Beer, M.A., McDonald, P.J., Rosales García, R.A., Rodriguez Lopez, B., Rubio Rincón, A., Franz Chávez, H., Vásquez-Cruz, V., Kelly Hernández, A., Storfer, A., Borja, M., Castañeda-Gaytán, G., Frandsen, P.B., Parkinson, C.L., Strickland, J.L., Margres, M.J., 2024. Where the "Ruber" meets the road: Using the genome of the red diamond rattlesnake to unravel the evolutionary processes driving venom evolution. Genome Biology Evol. 16 (9), evae198. http://dx.doi.org/10.1093/gbe/evae198.

Hirst, S.R., Vanhorn, C.M., Franz-Chávez, H., Vásquez-Cruz, V., Kelly-Hernández, A., Rosales-García, R.A., Castañeda-Gaytán, G., Borja, M., Parkinson, C.L., Strickland, J.L., Margres, M.J., 2026. Lack of an ontogenetic shift in crotalus enyo cerralvensis venom supports integration of cranial morphology and venom expression in rattlesnakes. West. North Am. Nat. 86 (1), 76–86. http://dx.doi.org/10.3398/064.086.0108.

Holding, M.L., Biardi, J.E., Gibbs, H.L., 2016. Coevolution of venom function and venom resistance in a rattlesnake predator and its squirrel prey. Proc. R. Soc. B: Biological Sci. 283 (1829), 20152841. http://dx.doi.org/10.1098/rspb.2015.2841.

Holding, M.L., Margres, M.J., Rokyta, D.R., Gibbs, H.L., 2018. Local prey community composition and genetic distance predict venom divergence among populations of the northern Pacific rattlesnake (Crotalus oreganus). J. Evol. Biol. 31 (10), 1513–1528. http://dx.doi.org/10.1111/jeb.13347.

Holding, M.L., Pontius, M.H.H., Ward, M.S., Akhtar, J., Crowell, H.L., Svilar, D., Keeler, K.M., Haynes, L.M., Ginsburg, D., Shavit, J.A., 2026. Deconstructing cardiovascular and coagulation-related traits links dietary ecology to multi-functional snake venom specificity. Evolution 80 (5), 1035–1046. http://dx.doi.org/10.1093/evolut/qpag036.

Holding, M.L., Strickland, J.L., Rautsaw, R.M., Hofmann, E.P., Mason, A.J., Hogan, M.P., Nystrom, G.S., Ellsworth, S.A., Colston, T.J., Borja, M., Castañeda-Gaytán, G., Grünwald, C.I., Jones, J.M., Freitas-de-Sousa, L.A., Viala, V.L., Margres, M.J., Hingst-Zaher, E., Junqueira-de-Azevedo, I.L.M., Moura-da-Silva, A.M., Grazziotin, F.G., Gibbs, H.L., Rokyta, D.R., Parkinson, C.L., 2021. Phylogenetically diverse diets favor more complex venoms in North American pitvipers. Proc. Natl. Acad. Sci. 118 (17), e2015579118. http://dx.doi.org/10.1073/pnas.2015579118.

Holzer, M., Mackessy, S.P., 1996. An aqueous endpoint assay of snake venom phospholipase A2. Toxicon 34 (10), 1149–1155. http://dx.doi.org/10.1016/0041-0101(96)00057-8.

Jackson, T.N.W., Fry, B.G., 2016. A tricky trait: Applying the fruits of the "Function Debate" in the philosophy of biology to the "Venom Debate" in the science of toxinology. Toxins 8 (9), 263. http://dx.doi.org/10.3390/toxins8090263.

Jackson, T.N.W., Koludarov, I., Ali, S.A., Dobson, J., Zdenek, C.N., Dashevsky, D., op den Brouw, B., Masci, P.P., Nouwens, A., Josh, P., Goldenberg, J., Cipriani, V., Hay, C., Hendrikx, I., Dunstan, N., Allen, L., Fry, B.G., 2016. Rapid radiations and the race to redundancy: An investigation of the evolution of Australian Elapid Snake Venoms. Toxins 8 (11), 309. http://dx.doi.org/10.3390/toxins8110309.

Kini, R.M., Koh, C.Y., 2016. Metalloproteases affecting blood coagulation, fibrinolysis and platelet aggregation from snake venoms: Definition and nomenclature of interaction sites. Toxins 8 (10), 284. http://dx.doi.org/10.3390/toxins8100284.

Lorke, D., 1983. A new approach to practical acute toxicity testing. Arch. Toxicol. 54 (4), 275–287. http://dx.doi.org/10.1007/BF01234480.

Lyons, W.J., 1971. Profound thrombocytopenia associated with Crotalus ruber ruber envenomation: A clinical case. Toxicon 9 (3), 237–240. http://dx.doi.org/10.1016/0041-0101(71)90075-4.

Mackessy, S.P., 1988. Venom ontogeny in the Pacific Rattlesnakes Crotalus viridis helleri and C. v. Oreganus. Copeia 1988 (1), 92–101. http://dx.doi.org/10.2307/1445927, arXiv:1445927.

Mackessy, S.P., 2010. Evolutionary trends in venom composition in the Western Rattlesnakes (*Crotalus Viridis* sensu lato): Toxicity vs. Tenderizers. Toxicon 55 (8), 1463–1474. http://dx.doi.org/10.1016/j.toxicon.2010.02.028.

Mackessy, S.P., 2021. Handbook of Venoms and Toxins of Reptiles. CRC Press.

Margres, M.J., Bigelow, A.T., Lemmon, E.M., Lemmon, A.R., Rokyta, D.R., 2017a. Selection to increase expression, not sequence diversity, precedes gene family origin and expansion in rattlesnake venom. Genetics 206 (3), 1569–1580. http://dx.doi.org/10.1534/genetics.117.202655.

Margres, M.J., McGivern, J.J., Seavy, M., Wray, K.P., Facente, J., Rokyta, D.R., 2015a. Contrasting modes and tempos of venom expression evolution in two snake species. Genetics 199 (1), 165–176. http://dx.doi.org/10.1534/genetics.114.172437.

Margres, M.J., McGivern, J.J., Wray, K.P., Seavy, M., Calvin, K., Rokyta, D.R., 2014. Linking the transcriptome and proteome to characterize the venom of the eastern diamondback rattlesnake (Crotalus adamanteus). J. Proteom. 96, 145–158. http://dx.doi.org/10.1016/j.jprot.2013.11.001.

Margres, M.J., Patton, A., Wray, K.P., Hassinger, A.T.B., Ward, M.J., Lemmon, E.M., Lemmon, A.R., Rokyta, D.R., 2019. Tipping the scales: The migration–selection balance leans toward selection in snake venoms. Mol. Biol. Evol. 36 (2), 271–282. http://dx.doi.org/10.1093/molbev/msy207.

Margres, M.J., Rautsaw, R.M., Strickland, J.L., Mason, A.J., Schramer, T.D., Hofmann, E.P., Stiers, E., Ellsworth, S.A., Nystrom, G.S., Hogan, M.P., Bartlett, D.A., Colston, T.J., Gilbert, D.M., Rokyta, D.R., Parkinson, C.L., 2021. The tiger rattlesnake genome reveals a complex genotype underlying a simple venom phenotype. Proc. Natl. Acad. Sci. 118 (4), e2014634118. http://dx.doi.org/10.1073/pnas.2014634118.

Margres, M.J., Walls, R., Suntravat, M., Lucena, S., Sánchez, E.E., Rokyta, D.R., 2016. Functional characterizations of venom phenotypes in the eastern diamondback rattlesnake (Crotalus Adamanteus) and evidence for expression-driven divergence in toxic activities among populations. Toxicon 119, 28–38. http://dx.doi.org/10.1016/j.toxicon.2016.05.005.

Margres, M.J., Wray, K.P., Hassinger, A.T.B., Ward, M.J., McGivern, J.J., Moriarty Lemmon, E., Lemmon, A.R., Rokyta, D.R., 2017b. Quantity, not quality: Rapid adaptation in a polygenic trait proceeded exclusively through expression differentiation. Mol. Biol. Evol. 34 (12), 3099–3110. http://dx.doi.org/10.1093/molbev/msx231.

Margres, M.J., Wray, K.P., Seavy, M., McGivern, J.J., Sanader, D., Rokyta, D.R., 2015b. Phenotypic integration in the feeding system of the eastern diamondback rattlesnake (Crotalus adamanteus). Mol. Ecol. 24 (13), 3405–3420. http://dx.doi.org/10.1111/mec.13240.

Massey, D.J., Calvete, J.J., Sánchez, E.E., Sanz, L., Richards, K., Curtis, R., Boesen, K., 2012. Venom variability and envenoming severity outcomes of the Crotalus Scutulatus Scutulatus (Mojave rattlesnake) from Southern Arizona. J. Proteom. 75 (9), 2576–2587. http://dx.doi.org/10.1016/j.jprot.2012.02.035.

Meik, J.M., Schaack, S., Flores-Villela, O., Streicher, J.W., 2018. Integrative taxonomy at the nexus of population divergence and speciation in insular speckled rattlesnakes. J. Nat. Hist. 52 (13–16), 989–1016. http://dx.doi.org/10.1080/00222933.2018.1429689.

Meik, J.M., Streicher, J.W., Lawing, A.M., Flores-Villela, O., Fujita, M.K., 2015. Limitations of climatic data for inferring species boundaries: Insights from speckled rattlesnakes. PLoS One 10 (6), e0131435. http://dx.doi.org/10.1371/journal.pone.0131435.

Minton, S.A., Weinstein, S.A., 1986. Geographic and ontogenic variation in venom of the western diamondback rattlesnake (Crotalus atrox). Toxicon 24 (1), 71–80. http://dx.doi.org/10.1016/0041-0101(86)90167-4.

Modahl, C.M., Mukherjee, A.K., Mackessy, S.P., 2016. An analysis of venom ontogeny and prey-specific toxicity in the Monocled Cobra (Naja kaouthia). Toxicon 119, 8–20. http://dx.doi.org/10.1016/j.toxicon.2016.04.049.

Mukherjee, A.K., Kalita, B., Mackessy, S.P., 2016. A proteomic analysis of Pakistan *Daboia Russelii Russelii* venom and assessment of potency of Indian polyvalent and monovalent antivenom. J. Proteom. 144, 73–86. http://dx.doi.org/10.1016/j.jprot.2016.06.001.

Munawar, A., Ali, S.A., Akrem, A., Betzel, C., 2018. Snake venom peptides: Tools of biodiscovery. Toxins 10 (11), 474. http://dx.doi.org/10.3390/toxins10110474.

Musick, S., Mann, N., Margres, M.J., Solis Solis, S.S., Parkinson, C., 2024. Fab antivenom reversal of neurotoxicity caused by a juvenile crotalus horridus lacking canebrake toxin. Wilderness Environ. Med. 35 (3), 342–346. http://dx.doi.org/10.1177/10806032241253823.

Neri-Castro, E., Lomonte, B., Valdés, M., Ponce-López, R., Bénard-Valle, M., Borja, M., Strickland, J.L., Jones, J.M., Grünwald, C., Zamudio, F., Alagón, A., 2019. Venom characterization of the three species of *Ophryacus* and proteomic profiling of *O. Sphenophrys* unveils Sphenotoxin, a novel Crotoxin-like heterodimeric β-neurotoxin. J. Proteom. 192, 196–207. http://dx.doi.org/10.1016/j.jprot.2018.09.002.

Neri-Castro, E., Zarzosa, V., Colis-Torres, A., Fry, B.G., Olvera-Rodríguez, A., Jones, J., Reyes-Velasco, J., Zamudio, F., Borja, M., Alagón, A., Lomonte, B., 2022. Proteomic and toxicological characterization of the venoms of the most enigmatic group of rattlesnakes: The long-tailed rattlesnakes. Biochimie 202, 226–236. http://dx.doi.org/10.1016/j.biochi.2022.08.015.

Oksanen, J., Blanchet, F.G., Friendly, M., Kindt, R., Legendre, P., McGlinn, D., Minchin, P., O'Hara, R.B., Simpson, G., Solymos, P., Stevens, M.H.H., Szöcs, E., Wagner, H., 2020. Vegan Community Ecology Package Version 2.5-7 November 2020.

Olmos-Martínez, E., Arizpe Covarrubias, O.A., Maldonado-Alcudia, C.M., Roldán-Clarà, B., 2018. Conservation of biodiversity vs tourism and fishing at the archipelago espiritu santo in the Gulf of California. In: Ortega-Rubio, A. (Ed.), Mexican Natural Resources Management and Biodiversity Conservation: Recent Case Studies. Springer International Publishing, Cham, pp. 501–517. http://dx.doi.org/10.1007/978-3-319-90584-6_22.

Pla, D., Sanz, L., Quesada-Bernat, S., Villalta, M., Baal, J., Chowdhury, M.A.W., León, G., Gutiérrez, J.M., Kuch, U., Calvete, J.J., 2019. Phylovenomics of Daboia russelii across the Indian subcontinent. Bioactivities and comparative in vivo neutralization and in vitro third-generation antivenomics of antivenoms against venoms from India, Bangladesh and Sri Lanka. J. Proteom. 207, 103443. http://dx.doi.org/10.1016/j.jprot.2019.103443.

Ponce-López, R., Neri-Castro, E., Borja, M., Strickland, J.L., Alagón, A., 2020. Neutralizing potency and immunochemical evaluation of an anti-*Crotalus Mictlantecuhtli* experimental serum. Toxicon 187, 171–180. http://dx.doi.org/10.1016/j.toxicon.2020.08.026.

Pozas-Ocampo, I.F., Carbajal-Saucedo, A., Gatica-Colima, A.B., Cordero-Tapia, A., Arnaud-Franco, G., 2020. Toxicological comparison of Crotalus ruber lucasensis venom from different ecoregions of the Baja California Peninsula. Toxicon 187, 111–115. http://dx.doi.org/10.1016/j.toxicon.2020.08.029.

Pucca, M.B., Ahmadi, S., Cerni, F.A., Ledsgaard, L., Sørensen, C.V., McGeoghan, F.T.S., Stewart, T., Schoof, E., Lomonte, B., auf dem Keller, U., Arantes, E.C., Çalışkan, F., Laustsen, A.H., 2020. Unity makes strength: Exploring intraspecies and interspecies toxin synergism between phospholipases A2 and cytotoxins. Front. Pharmacol. 11, http://dx.doi.org/10.3389/fphar.2020.00611.

R Core Team, 2024. R: A Language and Environment for Statistical Computing. R Foundation for Statistical Computing, Vienna, Austria, URL https://www.R-project.org/.

Rangel-Camacho, R., Yáñez-Arenas, C., Chippaux, J.P., Martín, G., 2025. Socioeconomic and ecological drivers of snakebite incidence in Mexico: A spatial analysis of risk factors. PLOS Neglected Trop. Dis. 19 (10), e0013582. http://dx.doi.org/10.1371/journal.pntd.0013582.

Ratanabanangkoon, K., 2003. Merit and demerit of polyvalent snake antivenoms. J. Toxicol.: Toxin Rev. 22 (1), 77–89. http://dx.doi.org/10.1081/TXR-120019563.

Ratanabanangkoon, K., 2023. Polyvalent snake antivenoms: Production strategy and their therapeutic benefits. Toxins 15 (9), 517. http://dx.doi.org/10.3390/toxins15090517.

Rodríguez-Canseco, J.M., Arnaud-Franco, G., Gutiérrez-López, E., Romero-Figueroa, G., 2021. Epidemiological overview of snakebites in the Baja California peninsula, Mexico (2003–2018). Gac. Med. Mex. 157 (6), 559–565. http://dx.doi.org/10.24875/GMM.M21000617.

Rokyta, D.R., Margres, M.J., Ward, M.J., Sanchez, E.E., 2017. The genetics of venom ontogeny in the eastern diamondback rattlesnake (Crotalus adamanteus). PeerJ 5, e3249. http://dx.doi.org/10.7717/peerj.3249.

Rokyta, D.R., Wray, K.P., Margres, M.J., 2013. The genesis of an exceptionally lethal venom in the timber rattlesnake (Crotalus Horridus) revealed through comparative venom-gland transcriptomics. BMC Genomics 14 (1), 394. http://dx.doi.org/10.1186/1471-2164-14-394.

Roldán-Padrón, O., Castro-Guillén, J.L., García-Arredondo, J.A., Cruz-Pérez, M.S., Díaz-Peña, L.F., Saldaña, C., Blanco-Labra, A., García-Gasca, T., 2019. Snake venom hemotoxic enzymes: biochemical comparison between crotalus species from Central Mexico. Molecules 24 (8), 1489. http://dx.doi.org/10.3390/molecules24081489.

Rudresha, G.V., Bhatia, S., Samanta, A., Nayak, M., Sunagar, K., 2025. Dissecting *Daboia*: Investigating synergistic effects of Russell's viper venom toxins. Int. J. Biiol. Macromol. 321, 146533. http://dx.doi.org/10.1016/j.ijbiomac.2025.146533.

Sanchez, E.F., Flores-Ortiz, R.J., Alvarenga, V.G., Eble, J.A., 2017. Direct fibrinolytic snake venom metalloproteinases affecting hemostasis: Structural, biochemical features and therapeutic potential. Toxins 9 (12), 392. http://dx.doi.org/10.3390/toxins9120392.

Sánchez, E.E., Galán, J.A., Perez, J.C., Rodríguez-Acosta, A., Chase, P.B., Pérez, J.C., 2003. The efficacy of two antivenoms against the venom of North American snakes. Toxicon 41 (3), 357–365. http://dx.doi.org/10.1016/S0041-0101(02)00330-6.

Schmitz, M.F., Diaz, P., 2013. Tourism as a Challenge. WIT Press.

Schonour, R.B., Huff, E.M., Holding, M.L., Claunch, N.M., Ellsworth, S.A., Hogan, M.P., Wray, K., McGivern, J., Margres, M.J., Colston, T.J., Rokyta, D.R., 2020. Gradual and discrete ontogenetic shifts in rattlesnake venom composition and assessment of hormonal and ecological correlates. Toxins 12 (10), 659. http://dx.doi.org/10.3390/toxins12100659.

Secretaría de Salud, 2012. NOM-036-SSA2-2012, Prevención y control de enfermedades. Aplicación de vacunas, toxoides, faboterápicos e inmunoglobulinas en el humano.

Senji Laxme, R.R., Khochare, S., de Souza, H.F., Ahuja, B., Suranse, V., Martin, G., Whitaker, R., Sunagar, K., 2019. Beyond the 'Big Four': Venom profiling of the medically important yet neglected Indian snakes reveals disturbing antivenom deficiencies. PLoS Neglected Trop. Dis. 13 (12), e0007899. http://dx.doi.org/10.1371/journal.pntd.0007899.

Shannon, C.E., Weaver, W., 1998. The Mathematical Theory of Communication. University of Illinois Press.

Shimokawa, K.-i., Jia, L.-G., Wang, X.-M., Fox, J.W., 1996. Expression, activation, and processing of the recombinant snake venom metalloproteinase, Pro-Atrolysin E. Arch. Biochem. Biophys. 335 (2), 283–294. http://dx.doi.org/10.1006/abbi.1996.0509.

Smiley-Walters, S.A., Farrell, T.M., Gibbs, H.L., 2017. Evaluating local adaptation of a complex phenotype: Reciprocal tests of pigmy rattlesnake venoms on treefrog prey. Oecologia 184 (4), 739–748. http://dx.doi.org/10.1007/s00442-017-3882-8.

Smith, C.F., Nikolakis, Z.L., Ivey, K., Perry, B.W., Schield, D.R., Balchan, N.R., Parker, J., Hansen, K.C., Saviola, A.J., Castoe, T.A., Mackessy, S.P., 2023. Snakes on a plain: Biotic and abiotic factors determine venom compositional variation in a wide-ranging generalist rattlesnake. BMC Biol. 21 (1), 136. http://dx.doi.org/10.1186/s12915-023-01626-x.

Straight, R.C., glenn, J.L., Wolt, T.B., Wolfe, M.C., 1992. North-south regional variation in phospholipase a activity in the venom of crotalus ruber. Comp. Biochem. Physiol. B: Comp. Biochem. 103 (3), 635–639. http://dx.doi.org/10.1016/0305-0491(92)90382-2.

Strickland, J.L., Smith, C.F., Mason, A.J., Schield, D.R., Borja, M., Castañeda-Gaytán, G., Spencer, C.L., Smith, L.L., Trápaga, A., Bouzid, N.M., Campillo-García, G., Flores-Villela, O.A., Antonio-Rangel, D., Mackessy, S.P., Castoe, T.A., Rokyta, D.R., Parkinson, C.L., 2018. Evidence for divergent patterns of local selection driving venom variation in Mojave Rattlesnakes (Crotalus Scutulatus). Sci. Rep. 8 (1), 17622. http://dx.doi.org/10.1038/s41598-018-35810-9.

Swenson, S., Markland, F.S., 2005. Snake venom fibrin(ogen)olytic enzymes. Toxicon 45 (8), 1021–1039. http://dx.doi.org/10.1016/j.toxicon.2005.02.027.

Terra, R.M.S., Pinto, A.F.M., Guimarães, J.A., Fox, J.W., 2009. Proteomic profiling of snake venom metalloproteinases (SVMPs): Insights into venom induced pathology. Toxicon 54 (6), 836–844. http://dx.doi.org/10.1016/j.toxicon.2009.06.010.

Vohra, R., Cantrell, F., Williams, S., 2008. Fasciculations after rattlesnake envenomations: A retrospective statewide poison control system study. Clin. Toxicol. 46 (2), 117–121. http://dx.doi.org/10.1080/15563650701638925.

Wang, W.-J., Shih, C.-H., Huang, T.-F., 2004. A novel P-I class metalloproteinase with broad substrate-cleaving activity, agkislysin, from *Agkistrodon Acutus* venom. Biochem. Biophys. Res. Commun. 324 (1), 224–230. http://dx.doi.org/10.1016/j.bbrc.2004.09.031.

Warrell, D.A., 2010. Snake bite. Lancet 375 (9708), 77–88. http://dx.doi.org/10.1016/S0140-6736(09)61754-2.

Wolf, Y.I., Katsnelson, M.I., Koonin, E.V., 2018. Physical foundations of biological complexity. Proc. Natl. Acad. Sci. 115 (37), E8678–E8687. http://dx.doi.org/10.1073/pnas.1807890115.

Wray, K.P., Margres, M.J., Seavy, M., Rokyta, D.R., 2015. Early significant ontogenetic changes in snake venoms. Toxicon 96, 74–81. http://dx.doi.org/10.1016/j.toxicon.2015.01.010.

Xiong, S., Huang, C., 2018. Synergistic strategies of predominant toxins in snake venoms. Toxicol. Lett. 287, 142–154. http://dx.doi.org/10.1016/j.toxlet.2018.02.004.

Yamashita, K.M., Alves, A.F., Barbaro, K.C., Santoro, M.L., 2014. Bothrops jararaca venom metalloproteinases are essential for coagulopathy and increase plasma tissue factor levels during envenomation. PLOS Neglected Trop. Dis. 8 (5), e2814. http://dx.doi.org/10.1371/journal.pntd.0002814.

Zarzosa, V., Lomonte, B., Zamudio, F., Ponce-López, R., Olvera-Rodríguez, F., Borja, M., Alagón, A., Neri-Castro, E., 2024. Venom of the neotropical rattlesnake, *Crotalus Culminatus*: Intraspecific variation, neutralization by antivenoms, and immunogenicity in rabbits. Biochimie 216, 160–174. http://dx.doi.org/10.1016/j.biochi.2023.10.014.